Digital Classification of Landsat Data for Vegetation and Land-Cover Mapping in the Blackfoot River Watershed, Southeastern Idaho

DIGITAL CLASSIFICATION OF LANDSAT DATA FOR VEGETATION AND LAND-COVER MAPPING IN THE BLACKFOOT RIVER WATERSHED, SOUTHEASTERN IDAHO

Portion of the Preston 1:250,000 topographic map with insert of land cover information for the Blackfoot River watershed. Land cover was derived from digital classification of Landsat data (see fig. 16 for color display and explanation of land cover classes). The Landsat data have been registered to fit the topographic map, as shown by comparing the map detail with the land cover patterns.

Digital Classification of Landsat Data for Vegetation and Land-Cover Mapping in the Blackfoot River Watershed, Southeastern Idaho

By LAWRENCE R. PETTINGER

GEOLOGICAL SURVEY PROFESSIONAL PAPER 1219

A case study, including step-by-step procedures for computer-assisted analysis of Landsat digital data, with emphasis on assessment of classification accuracy and generation of output products

UNITED STATES GOVERNMENT PRINTING OFFICE, WASHINGTON: 1982

UNITED STATES DEPARTMENT OF THE INTERIOR

JAMES G. WATT, *Secretary*

GEOLOGICAL SURVEY

Dallas L. Peck, *Director*

Library of Congress Cataloging in Publication Data

Pettinger, Lawrence R.
Digital classification of Landsat data for vegetation and land-cover mapping in the Blackfoot River watershed, southeastern Idaho.

(Geological Survey professional paper; 1219)
Bibliography: p. 33
Supt. of Docs. no.: I 19.16:1219
1. Vegetation mapping–Remote sensing–Data processing. 2. Vegetation classification–Idaho–Blackfoot River watershed. 3. Botany–Idaho–Blackfoot River watershed. 4. Landsat satellites. 5. Blackfoot River watershed, Idaho. I. Title. II. Title: Classification of Landsat data for vegetation and land-cover mapping in the Blackfoot River watershed, southeastern Idaho. III. Title: Land-cover mapping in the Blackfoot River watershed, southeastern Idaho. IV. Series: United States. Geological Survey. Professional paper ; 1219.

QK63.P47 581.9'028 80-606816
AACR1

**For sale by the Distribution Branch, U.S. Geological Survey,
604 South Pickett Street, Alexandria, VA 22304**

CONTENTS

ILLUSTRATIONS

TABLES

DIGITAL CLASSIFICATION OF LANDSAT DATA FOR VEGETATION AND LAND-COVER MAPPING IN THE BLACKFOOT RIVER WATERSHED, SOUTHEASTERN IDAHO

By LAWRENCE R. PETTINGER

ABSTRACT

This paper documents the procedures, results, and final products of a digital analysis of Landsat data used to produce a vegetation and land-cover map of the Blackfoot River watershed in southeastern Idaho. Resource classes were identified at two levels of detail: generalized Level I classes (for example, forest land and wetland) and detailed Levels II and III classes (for example, conifer forest, aspen, wet meadow, and riparian hardwoods). Training set statistics were derived using a modified clustering approach. Environmental stratification that separated uplands from lowlands improved discrimination between resource classes having similar spectral signatures. Digital classification was performed using a maximum likelihood algorithm.

Classification accuracy was determined on a single-pixel basis from a random sample of 25-pixel blocks. These blocks were transferred to small-scale color-infrared aerial photographs, and the image area corresponding to each pixel was interpreted. Classification accuracy, expressed as percent agreement of digital classification and photointerpretation results, was 83.0± 2.1 percent (0.95 probability level) for generalized (Level I) classes and 52.2± 2.8 percent (0.95 probability level) for detailed (Levels II and III) classes.

After the classified images were geometrically corrected, two types of maps were produced of Level I and Levels II and III resource classes: color-coded maps at a 1:250,000 scale, and flatbed-plotter overlays at a 1:24,000 scale. The overlays are more useful because of their larger scale, familiar format to users, and compatibility with other types of topographic and thematic maps of the same scale.

INTRODUCTION

The objective of this study was to produce vegetation and land-cover maps using computer-assisted classification of Landsat digital data for the Blackfoot River watershed in southeastern Idaho. This report documents the analysis steps and presents examples of the final output products. The major steps involved in producing these maps were

1. Selection and preprocessing of Landsat computer-compatible-tape (CCT) data.
2. Compilation of a list of vegetation and land-cover types to be classified and mapped.
3. Selection of training areas and derivation of training statistics.
4. Testing of training statistics on test areas and comparing them with an independent interpretation of high-altitude color-infrared aerial photographs.
5. Classification of the watershed areas using a maximum likelihood classification algorithm.
6. Assessment of classification accuracy.
7. Geometric correction of classified images.
8. Generation of output products (an overlay to a 7½-minute topographic map and color-coded classified images at selected scales) and evaluation of their utility.

ACKNOWLEDGMENTS

The author is grateful for the advice and assistance given by many of his colleagues during this study. Special thanks go to Charles Nelson, of the EROS Data Center, for help in defining analysis procedures, evaluating results, and assisting in IDIMS operation. Especially critical and helpful manuscript reviews were provided by Charles Nelson, David Carneggie, and William Draeger, of the EROS Data Center, and Claire Hay, of the Remote Sensing Research Program, University of California, Berkeley. James Sturdevant, EROS Data Center, provided assistance in field data collection.

BACKGROUND

PREVIOUS-STUDY RESULTS

In a previous study of the Blackfoot River watershed (Carneggie and Holm, 1977), manual analysis of high-altitude color-infrared aerial photographs and a Landsat color-composite image was performed to demonstrate how remote-sensing techniques might yield information for preparing resource inventories and for monitoring land-cover changes. In 1976, the U.S. Geological Survey completed an environmental-impact statement (EIS) that documented impacts that could result from proposals to increase the rate of phosphate strip mining (U.S. Geological Survey, 1976). The objectives of the study by Carneggie and Holm were to demonstrate and identify practical remote-sensing approaches for (1) gathering information to be included in EIS preparation

and (2) monitoring subsequent environmental impacts resulting from phosphate strip mining.

DESCRIPTION OF THE STUDY AREA

The study area is the Blackfoot River watershed, Caribou County, southeastern Idaho (fig. 1). The area, as classified by the Soil Conservation Service (Austin, 1965), is part of the Northern Rocky Mountain Land Resource Area of the Rocky Mountain Range and Forest Region. The area is identified by the U.S. Forest Service (Bailey, 1976) as belonging to the Douglas-fir Forest Section of the Rocky Mountain Forest Province. Average annual precipitation in the area is 20–25 in. (510–640 mm), of which 50–60 percent falls as snow.

The topography of the watershed is varied and consists of a series of northwest- and southeast-trending ridges and valleys. Upland ridges average 7,700 ft (2,350 m) in altitude and contain phosphate-bearing rock. The ridges support conifer (lodgepole pine, Douglas-fir, and subalpine fir) and hardwood (aspen) forest species. Most of the upland areas are administered by the U.S. Forest Service, U.S. Bureau of Land Management, and State of Idaho Lands Department. Lowland areas average 6,250 ft (1,900 m) in altitude. A large part of the lowlands is privately owned and has been converted from shrubland to grassland in order to improve forage production. A list of common and Latin plant species names is given in the following table (Little, 1953; Munz and Keck, 1963):

Common name	Latin name
Aspen	*Populus tremuloides* Michx.
Big sagebrush	*Artemisia tridentata* Nutt.
Bitterbrush	*Purshia tridentata* (Pursh) DC.
Chokecherry	*Prunus virginiana* L.
Douglas-fir	*Pseudotsuga Menziesii* (Mirb.) Franco
Engelmann spruce	*Picea Engelmannii* Parry
Lodgepole pine	*Pinus contorta* Dougl.
Mountain-mahogany	*Cercocarpus* HBK.
Mountain maple	*Acer glabrum* Torr.
Rush	*Juncus* L.
Sedge	*Carex* L.
Serviceberry	*Amelanchier* Medic.
Snowberry	*Symphoricarpos* Duhamel.
Subalpine fir	*Abies lasiocarpa* (Hook.) Nutt.
Willow	*Salix* L.

The watershed is very sparsely settled; only a few ranches and five phosphate strip mines are permanent. However, hunting, fishing, camping, and other types of outdoor recreation bring numerous seasonal visitors to the area.

Wildlife values are considerable in the study area. Elk, moose, and deer occupy the upland slopes. The upper tributaries of the Blackfoot River are recognized as critical spawning grounds for cutthroat trout. Beaver reside in riparian areas. Greater sandhill cranes and other waterfowl nest in the bottomland meadows; sage, blue, and ruffed grouse live in the lowlands and forests.

The peregrine falcon, an endangered species, nests in the watershed. The whooping crane, another endangered species, has been introduced via the foster-parent program near the study area at Grays Lake National Wildlife Refuge. It is anticipated that these birds will follow their greater sandhill crane foster parents and eventually set up nesting territories in and around the refuge. Greater sandhill crane habitats in the valley bottoms of the watershed therefore are potential whooping crane habitats.

IDENTIFICATION OF RESOURCE CLASSES

The first step in the production of a vegetation and land-cover map is to define the cover classes to be mapped. The draft EIS vegetation classification (U.S. Geological Survey, 1976) served as the starting point for the construction of a classification scheme for the digital analysis. A previous manual and digital analysis of Landsat data for the study area (Carneggie and Holm, 1977, p. 253–256) used a more detailed vegetation-classification framework than did the draft EIS. Based on the draft EIS and this previous study, resource classes listed in table 1 were defined.

The vegetation and land-cover categories are presented in a hierarchical framework similar to the one proposed by Anderson and others (1976) and adopted by the U.S. Geological Survey. Where appropriate, the same Levels I and II land-cover class names are used so that direct comparison can be made with other studies that use the U.S. Geological Survey system of classification. Note that more than one half of the proposed categories are defined as Level III in the hierarchy. Brief descriptions of the categories appear in table 2.

SELECTION OF REMOTELY SENSED DATA

During a previous manual analysis of a Landsat image of the study area, Carneggie and Holm (1977) concluded that a Landsat image acquired in the late-summer season (August-September) was best for distinguishing the major vegetation-cover types (conifer and hardwood forest, sagebrush–perennial grassland, and meadow). At the time images were selected for this study, the most recent high-quality, cloud-free, late-summer Landsat image had been acquired on August 15, 1974 (fig. 2). Data from the multispectral scanner (MSS) of Landsat 1 were chosen for this analysis.

In addition to Landsat data, aerial photographs were required for training-set evaluation and accuracy assessment. High-altitude color-infrared aerial photographs had been acquired by the National Aeronautics and Space Administration (NASA) on August 26, 1975.

TABLE 1.—*Comparison of resource classes selected for digital analysis with classes used in the southeastern Idaho draft EIS*

Resource classes from draft EIS [1]	Resource classes selected for digital analysis		
	Level I	Level II	Level III
Conifer and Aspen	Forest land	Conifer	
		Hardwood	Aspen
		Mixed conifer and hardwood	Mixed conifer and aspen
Mountain brush and sagebrush-perennial grass.	Rangeland	Mixed rangeland	Tall shrub
			Low shrub (upland, undisturbed)
			Low shrub (lowland, undisturbed)
			Low shrub (lowland, disturbed)
Riparian (sedges, rushes, willows).	Wetland	Nonforested wetland	Wet meadow
			Dry meadow
		Forested wetland	Riparian hardwoods
Marshlands (emergent and submergent vegetation in areas inundated during most of the growing season; for example, Grays Lake).	(None in watershed area.)	None	None
Agriculture (small grains, some alfalfa hay, grass, and pasture).	Agricultural land	Cropland and pasture	
Water	Water	Reservoirs	
Roads	Barren land	Strip mines, roads, other disturbed land	
Urban development	(None in watershed area)	None	None

[1] U.S. Geological Survey (1976, v. I, p. 1–174 to 1–190).

Although there was a 1-year difference between the two image dates, the seasonal state was the same, and the 1-year difference could be tolerated. Some differences in vegetation state were anticipated (mainly due to differences in grazing intensity in the valley bottoms), but these were not considered to be a serious deterrent to a successful comparison of the two image sets.

In summary, the following images were used for the study:

Image type	*Date acquired*	*Image identification number*
Landsat MSS	August 15, 1974	81753173225G0.
NASA aircraft	August 26, 1975	5750022007ROLL, frames 6497–6500 and 6525–6528.

DESCRIPTION OF DIGITAL IMAGE ANALYSIS SYSTEM

The digital analysis reported here was performed at the EROS Data Center using the Interactive Digital Image Manipulation System (IDIMS), which is manufactured by Electromagnetic Systems Laboratories (ESL), Inc.[1]

Digital images are entered into the system from magnetic tapes. Analysts communicate with the system by means of typewriter terminals. Because the system can process more than one program at one time, multiple terminals are used for concurrent analysis sessions. Processing is done by a Hewlett Packard HP3000 minicomputer augmented by a core memory and moving-head disks.

Program outputs can be displayed or recorded in three different ways:

1. *Line printer or operator terminal.* Numerical results can be listed or tabulated on either the analyst's terminal or the line printer. Image data can be represented by character symbols, using one symbol for each picture element (pixel) in the image.
2. *Color video display monitor.* Images can be displayed and viewed using the video monitor. Different types of black-and-white or color displays are possible. Landsat data can be displayed as false-color composite images (figs. 5, 8). Classification results can be displayed as color-coded images, in which each resource class appears in a distinctive color (figs. 5, 8).
3. *Magnetic tape.* Output images can be recorded on tape for future recall and analysis. These stored images can also be used as inputs to other systems (for example, to film recorders to produce high-quality film images or to flatbed plotters to produce scaled maps).

IDIMS analysis is facilitated by the effective manner in which the analyst can communicate via the terminal and can manipulate images on the video display. The analyst can use a variety of terminal commands to change color codings, annotate images, or recall other images from disk storage. With a movable cursor, he can outline or stratify image areas or can read the digital brightness values and row-column coordinates of individual Landsat pixels.

PREPROCESSING OF LANDSAT DATA

Radiometric anomalies in raw Landsat data are introduced by sensor miscalibration, data losses during transmission or recording, sensor saturation, and atmospheric attenuation. Digital analysis usually begins with certain preprocessing steps that compensate or correct for these anomalies. By using IDIMS software to restore or correct the data, subsequent classification results are improved. The most important radiometric

[1] Trade names and commercial enterprises or products are mentioned in this report solely for necessary information. No endorsement by the U.S. Geological Survey is implied.

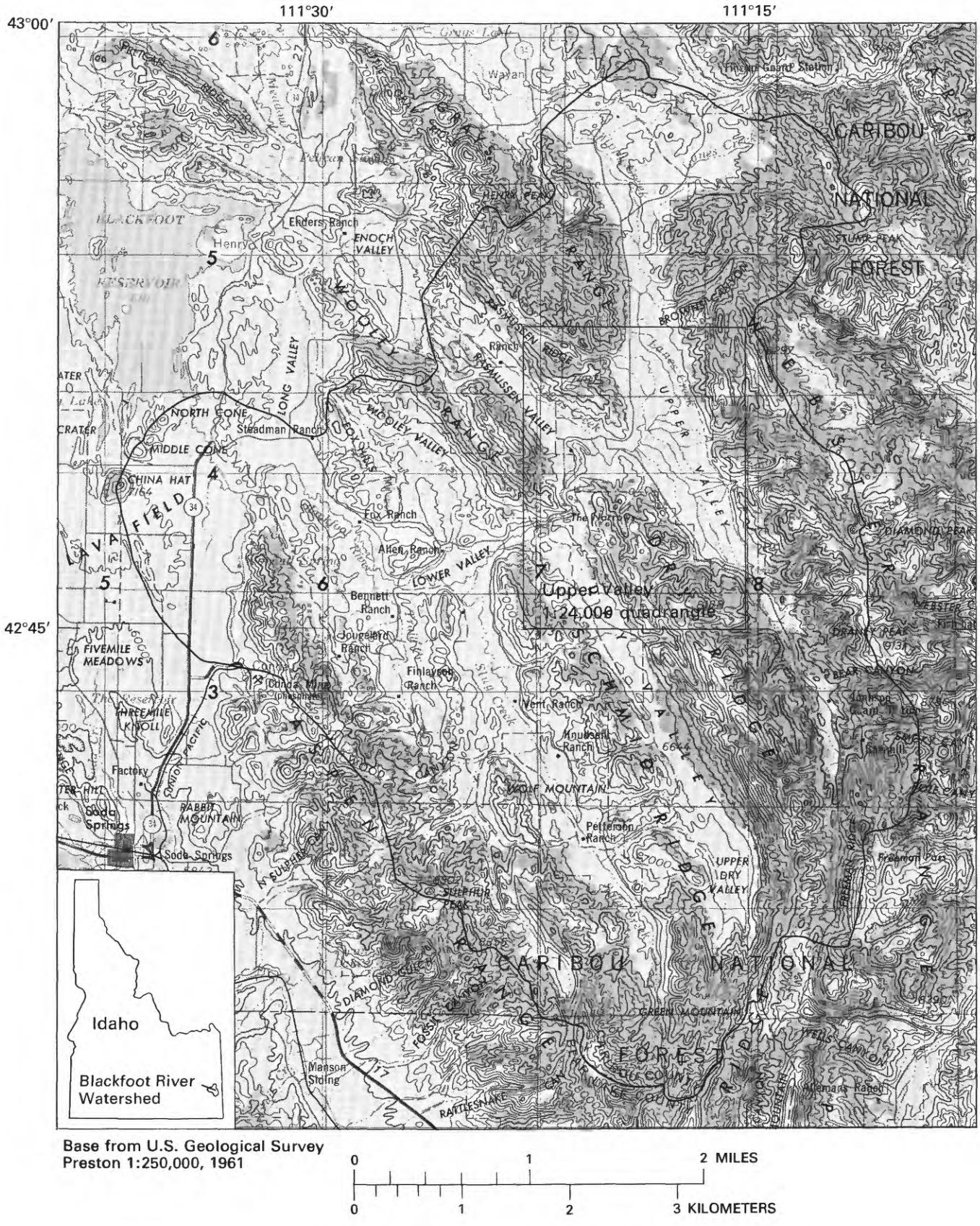

FIGURE 1.–Topographic map of part of southeastern Idaho, showing the Blackfoot River watershed.

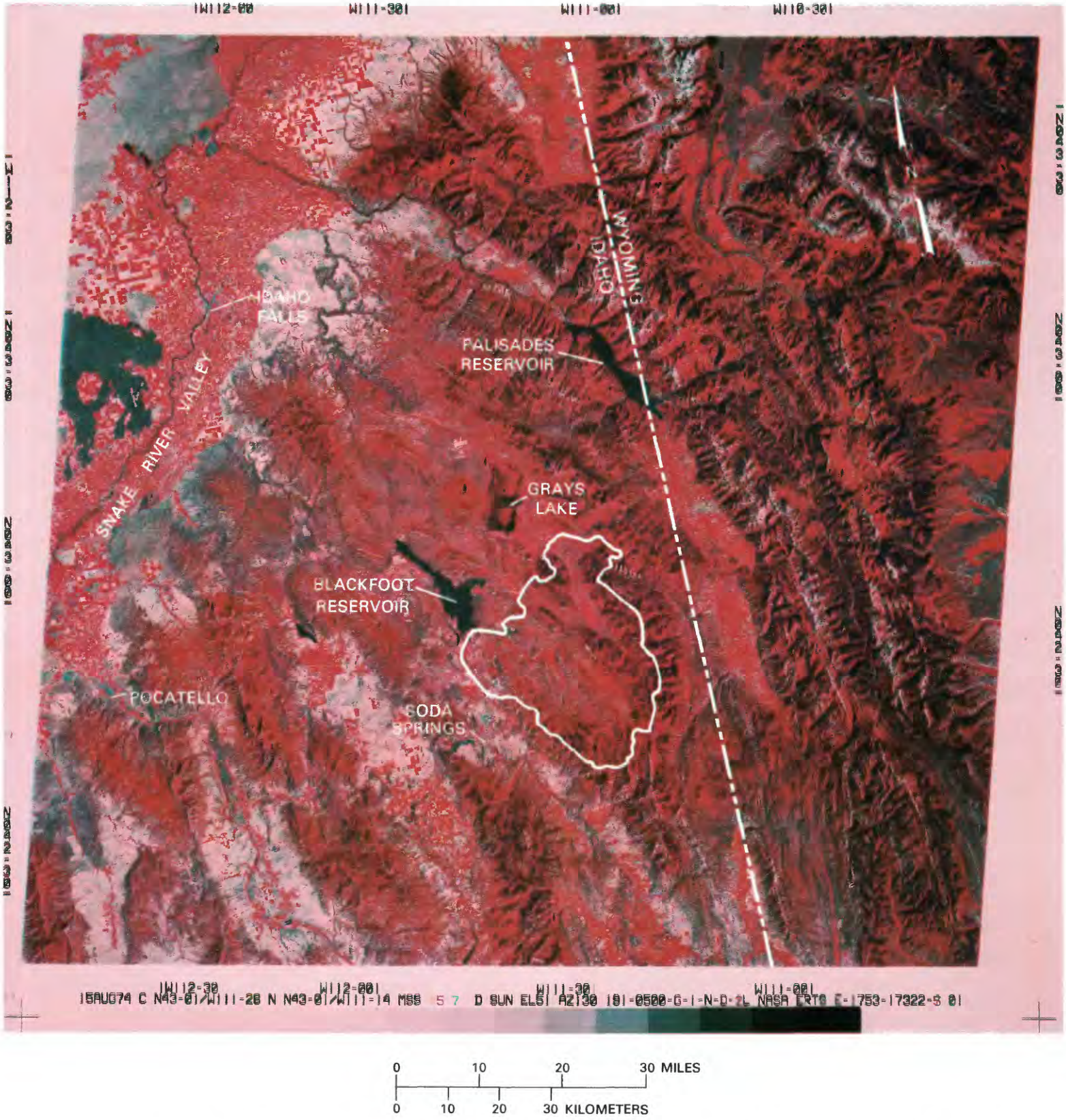

FIGURE 2. – Annotated Landsat color-composite image of part of southeastern Idaho and western Wyoming showing the outline of the Blackfoot River watershed (August 15, 1974; image identification number: 81753173225G0).

TABLE 2.—*Brief description of vegetation types defined for digital analysis in the Blackfoot River watershed*

Resource class	Species composition	General site characteristics
Conifer	Dominant overstory consists of lodgepole pine and Douglas-fir; Engelmann spruce and subalpine fir are minor constituents at higher altitudes.	Occurs most often on north- and east-facing upland slopes; at higher altitudes its occurrence is independent of aspect.
Aspen	Pure stands of aspen	Occurs in uplands on a variety of aspects.
Tall shrub	Dominant components include bitterbrush, serviceberry, snowberry, chokecherry, mountain maple, and mountain-mahogany.	Occurs on all aspects at lower altitudes; at higher altitudes, typically occurs on south- and west-facing slopes and ridge tops.
Low shrub (sagebrush-perennial grass).	Dominated by big sagebrush and a variety of perennial bunchgrasses; minor amounts of bitterbrush, serviceberry, and snowberry.	Generally occurs at lower altitudes than tall shrubs and on less productive soils; many lowland communities have been removed and the sites seeded with grasses to increase forage potential.
Wet/dry meadow	Sedges, rushes, and grasses	Occurs on moist valley bottoms; areas of denser vegetation are typically associated with moister sites.
Riparian hardwoods	Mixed willow species	Along banks of streams and ponds and in poorly drained canyon bottoms.
Cropland and pasture	Small grain crops, some alfalfa hay, grass, and pasture.	Occurs mostly on the Blackfoot Lava Field near the Blackfoot River Reservoir; elsewhere in a few valley-bottom locations.

corrections are made to eliminate striping or banding (caused by sensor miscalibration) and to replace bad-data lines (caused by dropouts of data during transmission and by sensor saturation).

RADIOMETRIC STRIPING

The Landsat MSS system, which has six detectors for each of the four spectral bands, scans six lines of data with each oscillation of the sensor mirror. Each detector has a slightly different response sensitivity to the incident radiation falling on it. As a result, the same intensity of incident radiation is not measured equally by each detector. The effect is known as striping or banding, and it appears on most standard-processed Landsat images. Striping contributes to errors in computer-aided classification and sometimes alters the spectral signatures of resource classes.

A common technique for minimizing striping—histogram normalization—was used in this study. In this method (HISTNORM algorithm), the mean brightness value for all pixels corresponding to each of the six detectors was calculated for each MSS band (a total of 24 mean values were calculated). A normalization (correction) factor was calculated by dividing the mean of the raw pixel values obtained from each detector into the mean of the detector having the lowest (minimum) value. New brightness values were assigned by multiplying the brightness value of each pixel by its detector's normalization factor. An example of the result of these calculations appears in table 3. Note that data from detector 3 of MSS band 4 data had the minimum mean. All normalization factors for band 4 were determined by dividing the mean relative radiance pixel value of detector 3 by each of the other detector means.

TABLE 3.—*Histogram normalization factors for reducing effect of radiometric striping anomalies*

[Data for MSS band 4 are shown; similar calculations were made for other MSS bands]

Detector	Mean of raw pixel values (relative radiance)	Normalization factor	Normalized mean pixel values (relative radiance)
1	26.8	0.948	25.4
2	26.5	.958	25.4
3	25.4	1.000	25.4
4	25.9	.981	25.4
5	26.2	.969	25.4
6	26.2	.969	25.4

BAD-DATA LINES

A second type of striping, known as intermittent striping or bad-data lines, is caused by dropouts of whole or partial lines of data or of single pixels. The most common causes are data losses during transmission and sensor saturation. Bad-data lines introduce random variations into the Landsat data and, if uncorrected, can lead to classification errors.

Bad-data lines were corrected using the FIXLINE algorithm. This algorithm replaces pixels from bad-data lines with the average of pixel values in the lines above and below the bad line. A new image is created that contains the corrected data lines.

DIGITAL MASK OF WATERSHED AREA

The corrected and normalized image was ready for the next analysis step, the selection of training areas. However, to reduce computer classification time, a digital mask corresponding to the Blackfoot River watershed boundary was applied to the preprocessed image. The mask restricted analysis to only the watershed area. The resulting masked image (fig. 3) was the

input image to the training and classification steps, which are described in subsequent sections.

DERIVATION OF TRAINING STATISTICS

OVERVIEW OF TRAINING APPROACHES

There are five steps in the Landsat digital classification process:

1. Define groups of Landsat pixels (training sets) that correspond to each of the resource classes in the classification scheme.
2. Calculate statistical parameters (training statistics) for each training set using a statistical computer algorithm.
3. Use the training statistics to "train" a digital classification algorithm.
4. Classify each Landsat pixel in the data set (in this case, the Blackfoot River watershed) into a computer class that represents a resource class.
5. Produce a color-coded resource map or other type of output product.

The accuracy of classification depends upon the degree to which spectral variability in the Landsat data is sampled during training-set selection. In the ideal situation, each resource class should be represented by one or more training sets that uniquely describe it; that is, there should be no confusion with other resource classes. Furthermore, the training sets should include examples of the range of spectral variability that can be expected throughout the study area.

There are two basic approaches to training-set selection: supervised and unsupervised training. The supervised approach to deriving training statistics was most commonly used in the early development of digital analysis techniques. This approach presumed that the analyst could select discrete image areas (training sets) that would correspond to each of the defined resource classes. The x-y image coordinates of these training sets would be specified to the computer, and training statistics would be generated for each resource class. This approach is called "supervised" training because the analyst selects specific areas that he knows contain a particular resource class.

Experience with this approach demonstrated that it was not satisfactory for environments where vegetation or land-cover types were complex or where there was great spectral variability within resource classes due to rugged terrain having great variation in slope and aspect. Because of such environmental variation, the analyst often had difficulty in selecting sufficient appropriate training areas to represent fully the range of variation in the data.

The alternative approach is termed "unsupervised" training. This approach presumes that spectral groupings within the Landsat data can best be determined by computer analysis. Using this approach, a random sample of training areas is selected without concern for the resource classes contained in each area. (Sample size is made large enough so that each resource class is adequately represented in the total sample.) All training-area pixels are combined, and a computer algorithm is used that separates the data into a prescribed number of groups of spectrally distinct pixels. This technique is often termed "clustering" to describe the way in which the computer algorithm forms these groupings or clusters of Landsat pixels.

After spectral clusters have been defined, the training process requires intensive man-machine interaction to correlate the clusters with the resource classes they represent. The approach is called "unsupervised" training because the analyst does not specify which Landsat pixels to use as training sets for each resource class. The random sample of pixels is assumed to contain a more representative sample of the spectral variability of the data than would a subjective supervised selection.

Variations of these two basic approaches to training have been devised. Using a "modified-supervised" approach, the analyst selects training sets for each of the known resource classes – the supervised method – but then he combines all the training sets and uses a clustering algorithm to separate the data into spectrally distinct classes. Resource-class names are then assigned by the analyst to each spectral cluster.

Another variation is called "modified unsupervised," "modified clustering," or "controlled clustering." The analyst selects several blocks of pixels (commonly 30-60 pixels square) that he believes contain representative examples of the range of spectral variability of the resource classes in the study area. Spectral clusters are defined by applying a clustering algorithm to the training data (either to the individual blocks or to an aggregation of blocks).

Fleming and others (1975) performed a test in which three of these four methods were compared. The results, expressed as percentage of correct classification of test fields in a wildland environment, were as follows:

Training method	*Percentage of correct classification*
Modified clustering	84.7
Unsupervised or clustering	78.5
Modified supervised	70.0

The modified (controlled) clustering approach was judged best because it resulted in savings of man-hours and computer time, as well as in the highest classification accuracy. The investigators concluded that the modified-clustering approach was especially well suited to spectrally complex areas having a variety of cover types and variable terrain.

TRAINING-AREA SELECTION

The modified-clustering approach was chosen for use in the present study because of its demonstrated utility in wildland environments (Fleming and others, 1975; Rohde and others, 1977, 1978). The Landsat-image characteristics of the resource types in the Blackfoot River watershed area were known from previous studies to be variable and to depend on steepness of slope and aspect; hence, it would be difficult to select completely representative training areas using a supervised-training approach.

Training areas were selected to include representative examples of the various resource classes in the watershed (fig. 3). Training areas were square or rectangular and were located so that several resource classes were included in each area. A total of seven areas were selected, which constituted a sample of 10 percent of the total watershed area.

CLUSTERING OF TRAINING-AREA DATA

The IDIMS clustering algorithm (ISOCLS) groups Landsat pixel values from the four MSS bands into relatively homogeneous clusters of pixels. The training areas can be clustered individually or grouped together and clustered as a whole. The latter approach was taken; the seven training areas were mosaicked to create a single 150- by 130-pixel training-area image (fig. 4). A considerable savings in time was achieved by evaluating one set of spectral clusters rather than seven.

The clustering algorithm operates by first assuming that all training pixels belong to one spectral cluster. This cluster is subdivided until the number, size, and separation distance of the clusters meet specified values. The specification of these parameters depends in part upon the spectral characteristics of the particular Landsat training set. The analyst must use his experience and knowledge of the area to select the clustering parameters. The parameters specified for this study are listed in table 4.

Each cluster is defined by a mean vector and a covariance matrix. The mean vector is the mean of the digital values of all pixels in the cluster in four-dimensional space, corresponding to the four Landsat MSS bands. The covariance matrix describes the spectral variability of the pixels about the mean and the covariance of the signature between spectral bands.

The output from the clustering algorithm consists of a statistics file (containing the mean and covariance for each cluster) and a new output image, called a clustered image. This image is a gray-level image in which each pixel of the mosaicked training areas is given the number corresponding to the spectral-cluster number to which the pixel is assigned.

TABLE 4.—*Algorithm parameters specified for IDIMS clustering of training-set data*

Parameter	ISOCLS nomenclature	Usual range	Specified value
Maximum number of iterations; that is, number of split or combine operations	ISTOP	15 -30	25
Minimum number of pixels (clusters with fewer than NMIN pixels will be deleted and their pixels assigned to other clusters)	NMIN	15 -30	30
Combining distance, Landsat relative radiance values (during a combining iteration, two clusters with mean < DLMIN will be combined)	DLMIN	2.5- 4.0	3.2
Maximum standard deviation (S.D.), Landsat relative radiance values (during a separating iteration, two clusters with S.D. > STDMAX and whose number of points is > 2(NMIN+1) will be split)	STDMAX	1.0- 3.0	2.5
Maximum number of clusters	MAXCLS	30 -60	50

TECHNIQUES FOR EVALUATING SPECTRAL CLUSTERS

The next analysis step is to assign a resource-class name to each of the spectral clusters and (if judged appropriate) to combine clusters that have very similar spectral characteristics and represent the same resource class. The desired result of cluster evaluation is a final set of spectral clusters and corresponding training statistics that will be the basis for classifying the entire image.

The steps for evaluating spectral clusters are as follows:

1. Display the clustered image of the training-area mosaic on a video display screen. Shades of gray represent the cluster assignments of each pixel.
2. Color-code single or multiple clusters to reveal their location and distribution.
3. Compare the color-coded cluster display with annotated aerial photographs or resource-class maps. Identify the resource class(es) that correspond to the display colors.
4. Reassign colors to clusters as necessary to effect the best possible match of spectral clusters with resource classes.

A color paper print of the Landsat color-composite image of the mosaicked training areas is useful for this comparison since the raw Landsat data cannot be displayed in color on the same IDIMS screen as the clustered image. The color-composite image is useful in visually comparing the clustered image with ground data because it is often difficult to relate the gray-scale values of the clusters directly to the ground data.

If a video display screen is not available, the clustered image can be produced in line printer map format. The character symbols on the line-printer map correspond to the spectral clusters, but they are more difficult to interpret and manipulate. Spectral clusters can be regrouped and displayed in different colors in a matter of seconds on the video display, whereas reassigning alphanumeric symbols and producing a new line-printer map requires considerably more time.

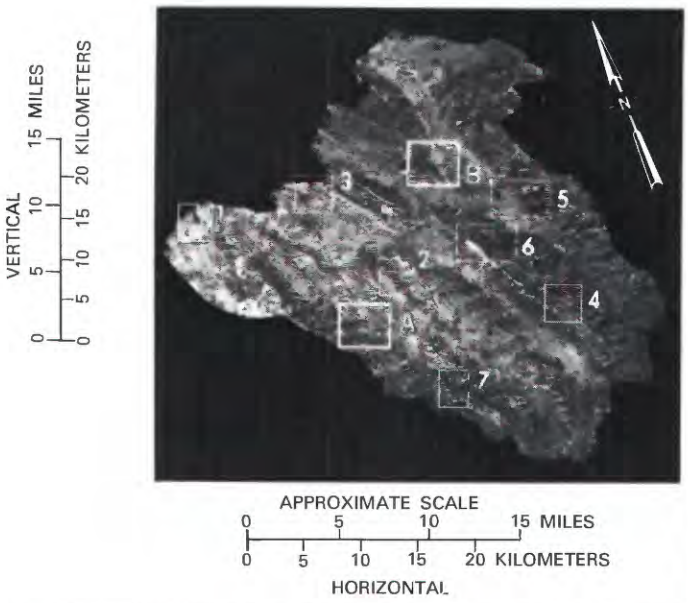

FIGURE 3.—IDIMS video display (not aspect corrected) of Landsat MSS band 5 image masked to show only the Blackfoot River watershed. Training areas are shown by letters (A, B), and test areas are shown by numbers (1-7).

The spatial relation of the spectral clusters also can be displayed as two-dimensional plots using the IDIMS COMPARE routine. The plots show the mean and standard deviation of each spectral cluster from any two MSS bands (fig. 7). These plots are a convenient base for assigning resource-class names to clusters or groups of clusters and for predicting which spectrally similar clusters might represent the same resource class.

Another aid in evaluating the similarity or differences between clusters is the IDIMS DIVERGE table, a matrix that expresses the distance in spectral space between each cluster and all others. This measure suggests which clusters are spectrally similar and might be combined and which are spectrally distinct and should be kept separate. The DIVERGE matrix should be used as a guide to manipulating clusters. Ground data, aerial photographs, and COMPARE plots should be used with the video display of the clustered image as the basis for making final cluster evaluations.

SPECTRAL-CLUSTER EVALUATION USING THE IDIMS VIDEO DISPLAY

Spectral clusters were evaluated using the video-display method described in the previous section. The technique is illustrated in figure 5. Preliminary analysis suggested that certain clusters represented conifer, aspen, or mixed conifer/aspen forest types (fig. 5*B*). These clusters were color coded on the clustered image (fig. 5*A*) and compared with the Landsat false-color

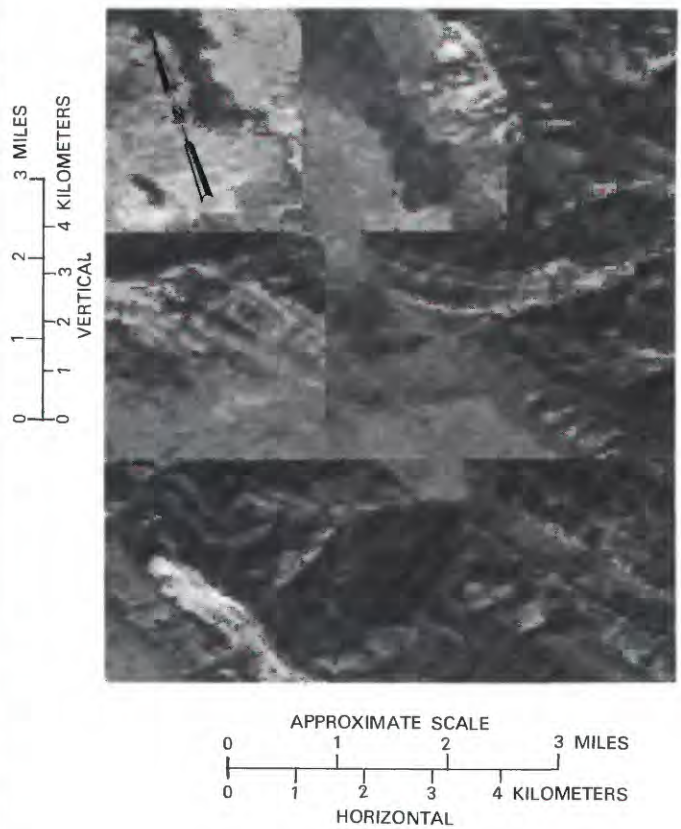

FIGURE 4.—IDIMS video display (not aspect corrected) of Landsat MSS band 5 image mosaic of training areas in the Blackfoot River watershed.

composite (fig. 5*C*) and with an annotated color-infrared aerial photograph of the same training area (fig. 5*D*). The selected clusters correlate well with conifer, aspen, and mixed conifer/aspen resource classes.

The presence of symbols for aspen (Fa) in the lowland (valley bottom) area where there is no aspen (red pixels on left side of image in fig. 5*A*) demonstrates that the spectral-reflectance values for aspen and wet meadow may overlap and that a potential for misclassification exists.

When the evaluation was completed, it was possible to associate a single resource class with certain clusters: conifer forest, water, and some sagebrush–perennial grass areas. However, in other clusters, the pixels correlated with more than one resource class. When spectrally similar pixels in a cluster represent two or more resource classes, there is spectral overlap between the classes. Spectral overlap was noted for the following groups of resource classes:

1. a. Aspen/wet meadow
   b. Aspen/dry meadow
   c. Aspen/riparian hardwoods

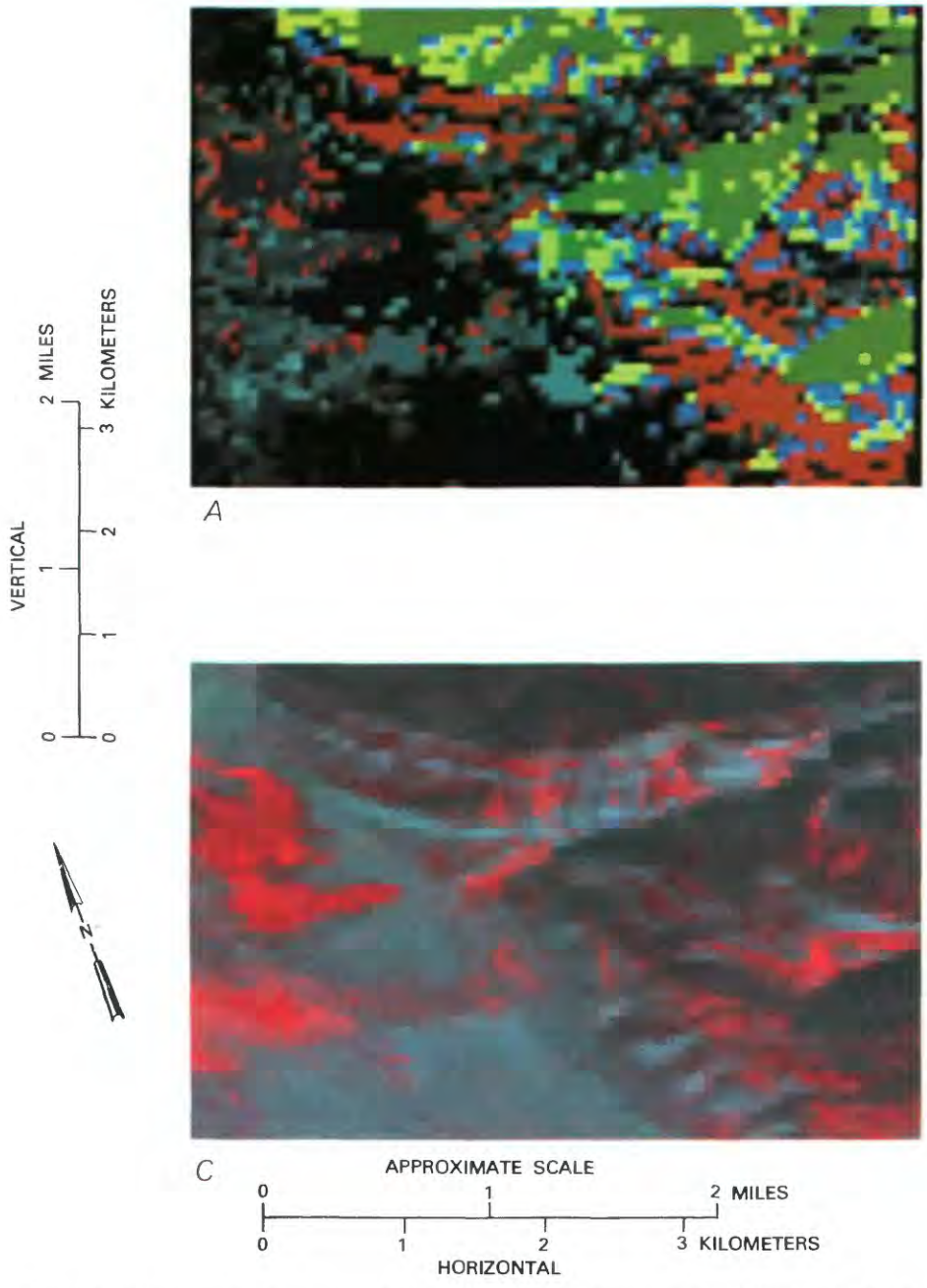

FIGURE 5.—Cluster evaluation process for training area 5. *A*, Color-coded IDIMS video display (not aspect corrected) of training area. Selected clusters have been color coded (green = **Fc**; red = **Fa**; yellow = **Fc/Fa**; blue = **Fa/Fc**). Uncolored clusters appear as various shades of gray. *B*, The outlined clusters in this COMPARE plot have been assigned to one of the forest resource classes (**Fc** = conifer; **Fa** = aspen; **Fc/Fa** = mixed, conifer predominates; **Fa/Fc** = mixed, aspen predominates). *C*, IDIMS video display (not aspect corrected) of Landsat false-color composite. Compare with *D*, Color-infrared aerial photograph of training area. Labels indicate location of selected conifer and aspen stands.

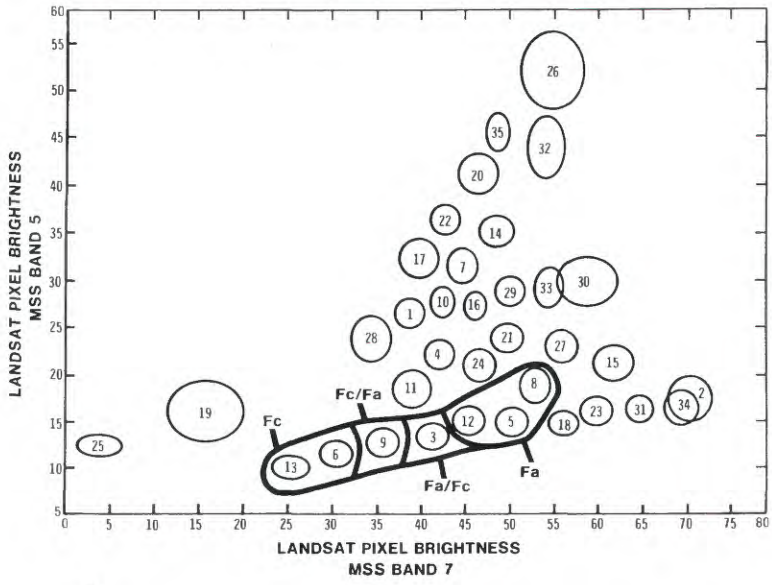

B

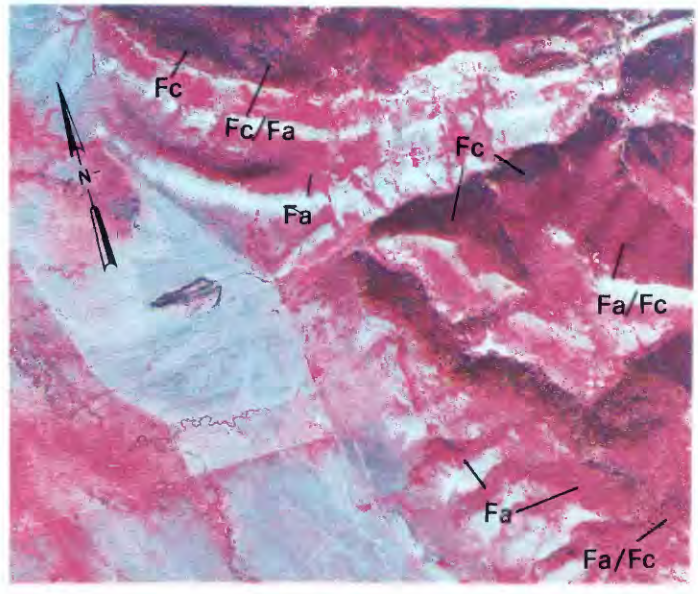

D

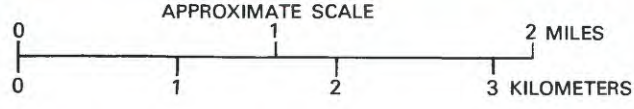

Figure 5.–Continued

2. a. Sagebrush–perennial grass (low density)/dry meadow
3. a. Sagebrush–perennial grass (low density)/roads and other disturbed areas/strip mines
   b. Sagebrush–perennial grass (very low density)/strip mines
4. a. Agricultural land/sagebrush–perennial grass (low and very low density)
   b. Agricultural land/roads and other disturbed areas
   c. Agricultural land/strip mines

The next section describes how environmental stratification was used to reduce potential misclassification because of spectral overlap.

ENVIRONMENTAL STRATIFICATION

The individual clusters for aspen, meadow, riparian hardwoods, sagebrush–perennial grass, and agricultural land could not be regrouped to resolve spectral overlap. Therefore, stratification was proposed to separate the resource classes by acknowledging that each resource class is associated with a unique, separable environmental stratum.

For example, the wet- and dry-meadow classes and riparian hardwoods are restricted to lowland environments, whereas aspen occurs only in the uplands. Lowland environments containing meadow or riparian-hardwood vegetation were delineated (stratified) on the IDIMS video display of the Landsat color-composite image (fig. 6). NASA color-infrared aerial photographs were a useful aid in the stratification process.

As might be expected, there were limitations to the extent that all lowland habitat could be stratified. For example, narrow, sinuous ribbons of riparian hardwoods were found in the stream bottoms in some upland areas. Aspen stands often abutted these narrow hardwood stands. Even though the IDIMS visual display was enlarged to show individual pixels clearly, it was difficult to distinguish some narrow stringers of riparian hardwoods from neighboring aspen stands. The overall effect in terms of number of pixels ignored (unstratified) or placed in the wrong stratum is small. However, these stringer stands often constitute valuable wildlife habitat, and such errors of omission might be significant.

The upland-lowland stratification helped to resolve a second type of spectral overlap, that between sagebrush–perennial grass (low density) and dry meadow. Most low-density sagebrush–perennial-grass areas occur on upland sites having shallow soils and low moisture availability. Dry meadows, on the other hand, are found in lowland environments adjacent to wet meadow and riparian sites. Thus, some low-density sagebrush–perennial-grass areas in the lowland stratum

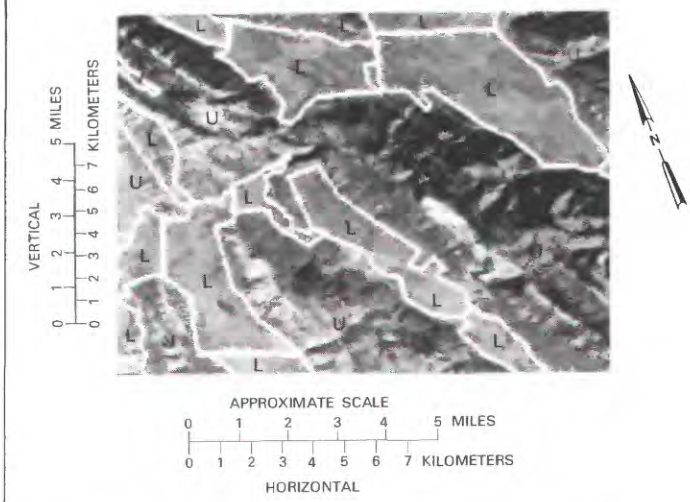

FIGURE 6.–IDIMS video display (not aspect corrected) of Landsat MSS band 5 image of a part of the Blackfoot River watershed showing upland (U)-lowland (L) environmental stratification (white lines). The lowland areas were stratified in segments because large areas having intricate shapes could not easily be stratified in a single operation on IDIMS.

might be incorrectly classified as dry meadow, but the overall effect of the stratification was judged to be useful in reducing spectral overlap.

A third type of spectral overlap was between sagebrush–perennial grass (low and very low density) and certain highly reflective features–strip mines, roads, and other disturbed areas. Examination of this type of spectral overlap revealed that there was no simple means of resolving this confusion. Therefore, it was decided that these clusters would be treated as a mixed resource class (sagebrush–perennial-grass/barren areas)–that is, unresolvable spectral overlap was accepted.

A fourth type of spectral overlap existed between agricultural land and sagebrush–perennial grass (low and very low density) and between agricultural land and highly reflective features. This overlap was caused by the similarity in reflectance of wheat stubble, low-density sagebrush–perennial grass, and barren areas. Since the only significant area of contiguous agricultural land occurs on the Blackfoot River Lava Field along Highway 34 in the northwest corner of the watershed it was possible to stratify this agricultural zone. Since there were no strip mines and few other cultural features (the Conda Mine and processing facility were carefully excluded) or low-density sagebrush–perennial-grass areas in this stratum, this operation was judged to improve the classification. Agricultural fields in other lowland environments were present, but their irregular

distribution, small size, and apparent lack of permanence from one year to another were factors considered in the decision not to perform agricultural stratification elsewhere in the watershed.

Figure 7 is a graphical representation of the clusters for which spectral overlap occurred. If a cluster has only one resource class label, that cluster represents only one resource class. Where two or more labels are given for a cluster, the resource class name is determined by the stratum (upland, lowland, or agricultural) where the cluster pixels were found.

FINAL DETERMINATION OF RESOURCE CLASSES

Table 5 contains the revised list of resource classes that resulted from the evaluation of spectral clusters. There are only two instances in which cluster evaluation resulted in changes in the resource-class name. The first instance was the deletion of the tall shrub category. As a result of cluster analysis, it was observed that vegetation communities composed of tall shrubs were small, irregular in shape, and in many places included aspen. It was very difficult to identify Landsat spectral clusters that correlated well with known tall-shrub areas in the training areas. As a result, tall shrub was deleted as a resource class. Because tall shrub and young aspen stands were spectrally similar, tall shrub stands in the watershed were probably classified as aspen.

The second change in resource-class name was in the low shrub category. This category was subdivided into four density levels rather than upland-lowland and disturbed-undisturbed sagebrush. These density levels were very low, low, medium, and high. The variation in Landsat relative-radiance levels for these classes correlates with the assigned density levels; that is, as vegetation density decreases (percentage of bare ground surface increases), Landsat MSS bands 5 and 7 (fig. 7) relative radiance increases. Comparison of Landsat image signatures with color-infrared aerial photographs of the study area revealed that patterns of herbicide spraying (the main type of activity causing the difference between disturbed and undisturbed sagebrush-perennial-grass communities) were not readily separable on the Landsat image. Hence, a category subdivision based on density was more realistic.

The final assignment of resource-class names to spectral clusters is given in table 5 and figure 7. For these assignments, environmental stratification of the watershed was made, separating (1) lowland sites from upland sites and (2) the zone of intensive agricultural land from the rest of the watershed.

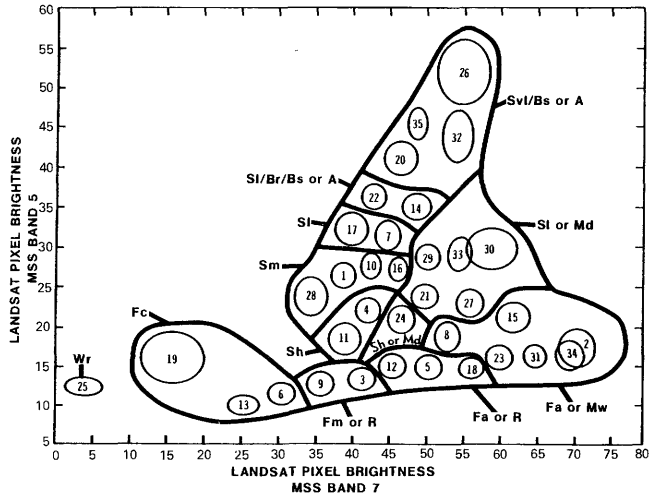

FIGURE 7.—Two-dimensional IDIMS COMPARE plot of spectral clusters obtained by clustering Landsat MSS data from training areas. Each numbered ellipse is the graphic representation of a spectral cluster; the mean value of the cluster lies at the center of the ellipse, and the ellipse boundary is drawn at a distance of one standard deviation from the mean. Heavy black lines surround a cluster or group of clusters to which a resource name or names have been assigned. Where a single resource-class symbol is given (Wr, Fc, Sh, Sm, Sl), there is no spectral overlap with another resource class. Where more than one resource-class symbol is shown for a cluster or group of clusters, the class symbol assigned is determined by the environmental stratum into which the pixels from the cluster or group of clusters fall, as follows: lowland stratum—R, Mw, Md, Svl/Bs, Sl/Br/Bs; upland stratum—Fm, Fa, Sl, Sh; agricultural stratum—A. See table 5 for explanation of resource-class symbols.

TABLE 5.—*Final determination of resource-class symbols and names for Level I and Levels II and III classifications*

Symbol		Name	
Level I	Levels II and III	Level I	Levels II and III
F		Forest land	
	Fc		Conifer
	Fa		Aspen
	Fm		Mixed conifer/aspen
S		Rangeland	
	Sh		Sagebrush-perennial grass (high density)
	Sm		Sagebrush-perennial grass (medium density)
	Sl		Sagebrush-perennial grass (low density)
T		Wetland	
	Mw		Wet meadow
	Md		Dry meadow
	R		Riparian hardwoods
S/B		Rangeland/ barren land	
	Sl/Br/Bs		Mix of sagebrush-perennial grass (low density)/strip mines/roads and other disturbed areas
	Svl/Bs		Mix of sagebrush-perennial grass (very low density)/strip mines
A		Agricultural land	
	Ac		Cropland and pasture
W		Water	
	Wr		Reservoirs

TESTING THE VALIDITY OF SPECTRAL-CLUSTER AND RESOURCE-CLASS ASSIGNMENTS PRIOR TO THE CLASSIFICATION OF THE ENTIRE WATERSHED AREA

GENERAL APPROACHES

Most digital-classification projects attempt to verify the validity of resource-class name assignments to spectral clusters on small test areas prior to classifying the entire project area. If there are resource classes having low classification accuracy, then one might (1) re-evaluate spectral clusters and reassign resource-class names, (2) change resource-class names to describe clusters that are spectrally distinct, (3) consider further environmental stratification, or (4) recluster the training data.

Two common approaches to testing classification accuracy are to (1) run the classification algorithm on the same training data that were used to derive the training statistics or (2) classify different test areas that are independent of the training areas. Although classification of the training area is commonly used, this approach can introduce bias that results in unrealistically high classification accuracy that cannot be attained for the entire area or even for other subareas.

TEST-AREA CLASSIFICATION

The training statistics were tested by classification of two test areas (fig. 3). These areas were representative of the study area and were independent of the training areas. Each test area measured 60 by 70 pixels, and contained 4,695 acres (1,900 ha). Together, the two test areas represent 4.2 percent of the entire watershed.

By means of the training statistics (mean, standard deviation, covariance) for the final cluster groupings that are graphically displayed in figure 7, test areas A and B were classified using the CLASFY routine on IDIMS. A color-coded display of the results for test area B appears in figure 8. A visual comparison of the false-color image (8*A*), the classification results (8*B*), and the corresponding high-altitude color-infrared aerial photograph (8*C*) shows good general agreement between the resource classes and classification results, both in terms of boundary location between classes and in class designations.

MANUAL PHOTO INTERPRETATION OF TEST AREAS

The visual comparison presented above is the same technique used earlier to qualitatively evaluate the training areas. To make a quantitative comparison, the following steps were taken:

1. Manual photo interpretation was performed for the part of the aerial photographs corresponding to test areas A and B.
2. The area occupied by each resource class was determined.
3. Area estimates from the photo interpretation and digital classification were compared for all resource classes.

The image analyst was familiar with the field characteristics of the resource classes and their color-infrared image signatures, but he was not involved in the digital classification. Prior to the photo interpretation, the author and the interpreter discussed the resource classes and their photographic signatures. The interpreter then proceeded with a stereoscopic analysis of the test areas using paper print enlargements of the aerial photographs at an approximate scale of 1:24,000. The minimum mapping unit was about 1.1 acre (0.44 ha), corresponding to the approximate size of one Landsat pixel. A copy of the photo-interpretation results at reduced scale appears in figure 8*D*.

EVALUATION OF TEST-AREA CLASSIFICATION RESULTS

Area determinations were made for each resource class using a dot grid. One dot-grid conversion factor

FIGURE 8.—Comparison of Landsat image (*A*) and digital classification image (*B*) (both from IDIMS video displays, not aspect-corrected) of test area B with corresponding high-altitude color-infrared aerial photograph (*C*) and vegetation map prepared from aerial photograph by manual interpretation (*D*). Dashed lines on *C* trace fences that separate areas of different grazing intensities. Note that the image signatures on *A* do not correspond exactly to the patterns on *C*, suggesting a change in grazing patterns between the time the Landsat image was acquired (August 15, 1974) and the time the high-altitude aerial photograph was taken (August 26, 1975).

EXPLANATION

Resource class	Type of classification: Digital	Type of classification: Manual
Forest land:		
Conifer	Purple	Fc
Aspen	Violet	Fa[1]
Mixed conifer/aspen	Gray	Fm
Rangeland:		
Sagebrush–perennial grass (high density)	Dark green	H
Sagebrush–perennial grass (medium density)	Light green	M
Sagebrush–perennial grass (low density)	Yellow	L
Sagebrush–perennial grass (very low density)	None	VL
Rangeland/barren land:		
Sagebrush–perennial grass (very low density)/strip mines	Light blue	B[2]
Sagebrush–perennial grass (low density)/strip mines/ other disturbed areas	Medium blue	B[2]
Wetland:		
Wet Meadow	Red	Mw[1]
Dry Meadow	Brown	Md
Riparian hardwoods	Black	R

[1]Shading added to map for emphasis.
[2]Barren areas only.

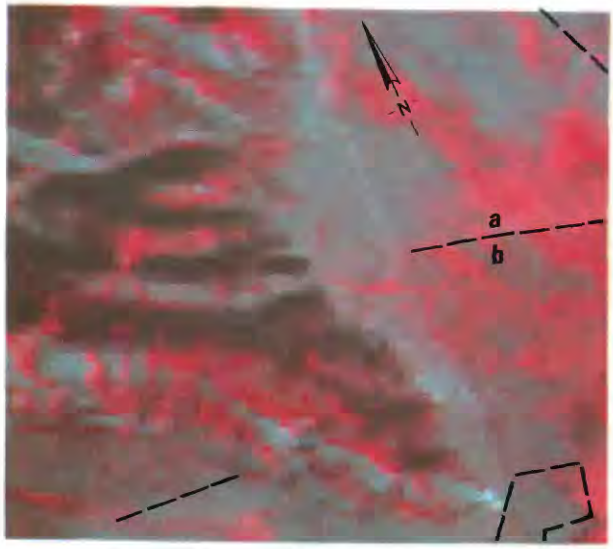
N
a
b

A

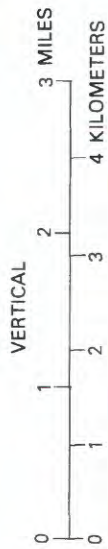
VERTICAL
0
1
2
3
3 MILES
4 KILOMETERS

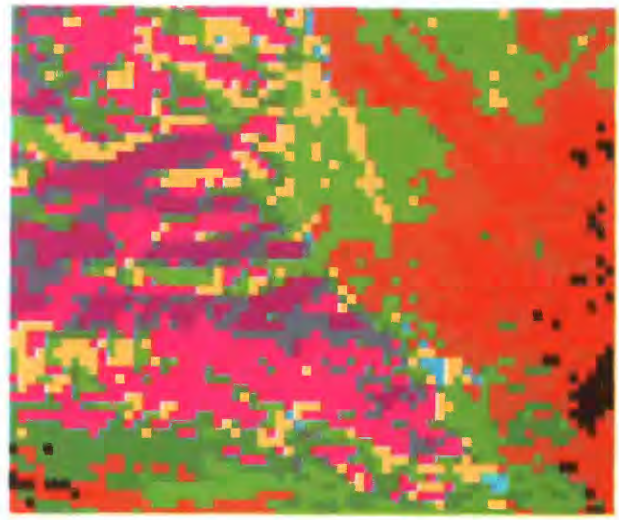

B

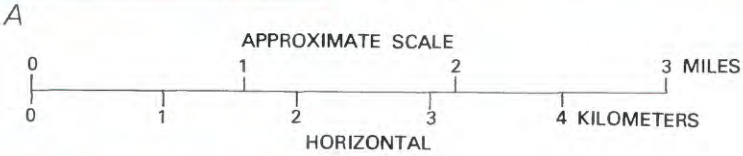
APPROXIMATE SCALE
0
1
2
3 MILES
0
1
2
3
4 KILOMETERS
HORIZONTAL

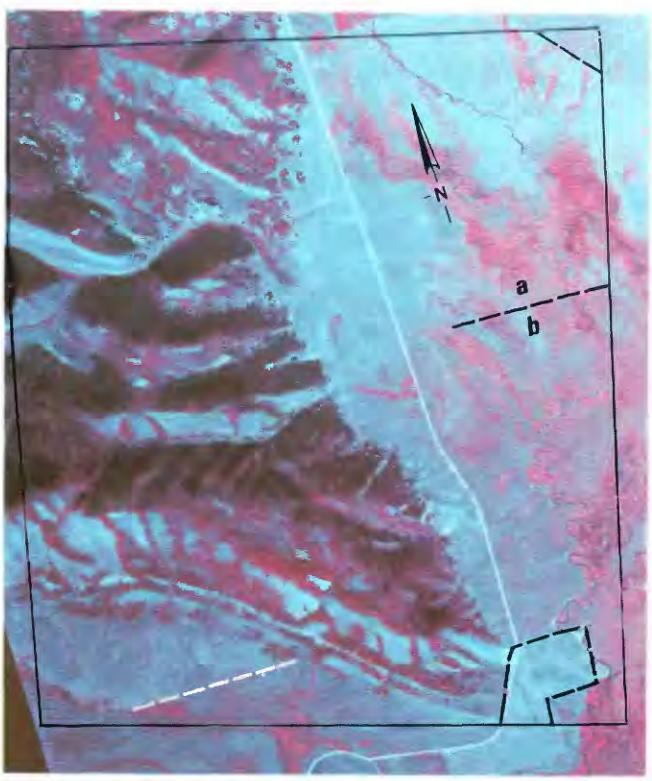
N
a
b

C

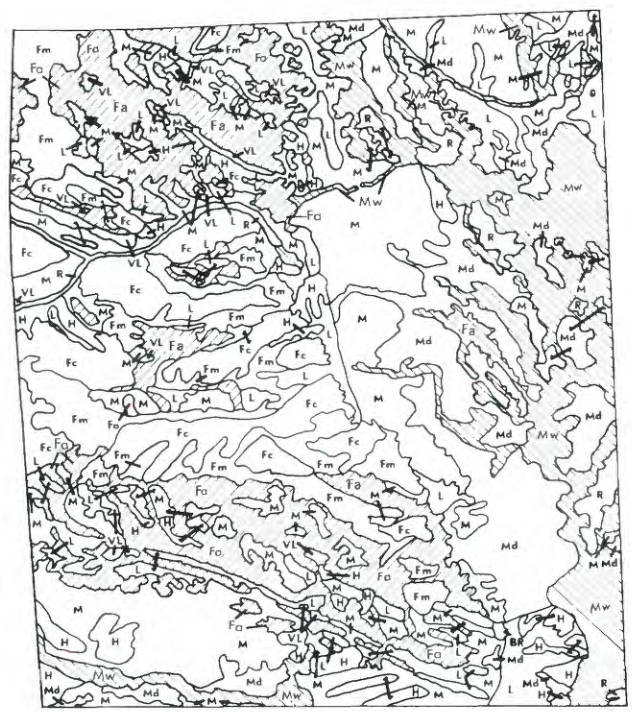

D

TABLE 6.—*Comparison of area estimates from manual photo interpretation and digital classification for test areas A and B*

Resource class	Area							
	Test area A				Test area B			
	Digital classification		Manual photo interpretation		Digital classification		Manual photo interpretation	
	Acres	Hectares	Acres	Hectares	Acres	Hectares	Acres	Hectares
Level I resource classes								
Forest land	1,471	596	1,649	668	1,362	551	1,641	664
Rangeland	2,523	1,021	2,453	993	1,985	804	1,718	696
Rangeland/barren land	166	67	33	13	31	13	33	13
Wetland	535	216	578	234	1,317	533	1,283	520
Total	4,695	1,900	[1]4,713	1908	4,695	1,901	[1]4,675	1893
Levels II and III resource classes								
Forest land:								
Fa	574	233	810	328	591	239	795	322
Fc	136	55	269	109	315	127	456	184
Fm	761	308	570	231	456	185	390	158
Rangeland:								
Sh	815	330	790	320	643	260	206	84
Sm	1,244	503	1,344	544	965	391	1,190	482
Sl	464	188	319	129	377	153	322	130
Rangeland/barren land:								
Sl/Br/Bs	122	49	[2]1	([3])	28	12	[2]2	1
Svl/Bs	44	18	[4]32	13	3	1	[4]31	12
Wetland:								
Md	325	131	178	72	743	301	522	212
Mw	160	65	346	140	481	195	674	273
R	50	20	54	22	93	37	87	35
Total	4,695	1,900	[1]4,713	1,908	4,695	1,901	[1]4,675	1,893

[1] Total area for test areas A and B from manual photo interpretation does not equal total area from digital classification because of (1) errors in precise transfer of test area boundaries from Landsat display to enlarged aerial photographs and (2) slight distortion in the size and shape of map units due to relief displacement in upland areas on the aerial photographs.

[2] Br only.

[3] Value less than 1.

[4] Svl only.

was calculated for each test area, using the scale calculated at the average altitude of the test-area terrain.

A simple correlation analysis (Walker and Lev, 1953, p. 233–255) was performed to test the correlation of digital classification with manual photo interpretation, using areas classified into the Levels II and III resource classes by these two approaches. Correlation coefficients (r) and confidence intervals (C.I., 95-percent probability level) were as follows:

Test area	*r*	*C.I.*
A	0.97	0.89–0.99
B	.94	.77– .98

The two data sets are highly correlated.

A comparison of manual and digital resource classification results is presented in table 6. Although a pixel-by-pixel accuracy assessment was made later in the study to assess classification accuracy for the whole area, an area-by-resource class comparison was used because it was less time consuming and still revealed areas of classification agreement and disagreement.

For the Level I (most general) classes in area B, the total areas computed for each of the two methods were similar. The only significant discrepancies—between areas for forest land and rangeland—probably resulted from the interspersion of small patches of rangeland with forest (mostly aspen) in the uplands. Digital separation of these two classes relied solely upon spectral differences, whereas the photo interpreter used stereoscopic analysis, as well as subtle tonal and textural differences, to make the distinction. Hence, some differences in the areas computed were anticipated for these classes.

When the Levels II and III classes in test area B are evaluated, the same conclusion regarding the complexity of the sagebrush–perennial-grass and forest classes applies. The largest discrepancies within the forest and sagebrush–perennial-grass classes were associated with aspen and high-density sagebrush–perennial grass. Clusters representing aspen and mixed conifer/aspen in upland areas (9, 3, 12, 5, 8) and high-density sagebrush–perennial grass (11, 4, 24) are spectrally similar (fig. 7). This spectral overlap may well contribute to differences in results between the two methods of analysis.

Although the total-area estimates from manual and digital analysis of the wetland (Level I) category are similar, when the wet- and dry-meadow components were studied at Levels II and III, a difference of approx-

imately 200 acres (80 ha) was revealed. Seasonal differences between 1974 and 1975 might explain this difference.

Differences in area estimates for the sagebrush–perennial-grass classes were also acknowledged. Close study of the image of this test area (fig. 8*A*, *C*) reveals change in grazing intensity between the 1974 and 1975 image dates. For example, grazing appears to have been heavier at *a* (lighter pink color) than at *b* in the 1974 Landsat image; in the 1975 aerial photograph, this difference is not so clear. Other examples are highlighted by the dashed lines on the two images.

Having evaluated these differences in seasonal state and grazing (in the wetland and sagebrush–perennial-grass communities) and complex interspersion of aspen and sagebrush–perennial grass (in the uplands) in test area B, similar differences can be noted in test area A (table 6) in both the Level I and Levels II and III resource classes. Again, seasonal and grazing differences and the complex interspersion of sagebrush–perennial grass and aspen seem to be the major factors in explaining the differences.

It was concluded that the spectral classes derived from the training areas were satisfactory for purposes of the classification. It should be pointed out that even though the aerial photographs were of greater resolution than the Landsat image, photo interpretation could not be accepted as the equivalent of complete field verification because of the 1-year interval between the two sets of images. Although manual photo interpretation of sagebrush–perennial-grass/aspen boundaries is probably more accurate than the digital classification, the relative accuracy of the sagebrush–perennial-grass density and wet/dry meadow classes cannot be assessed on a class-by-class basis because of the different livestock grazing patterns that have been imposed on the watershed in the 2 years.

Based on the relatively close agreement in Level I acreage estimates from manual and digital analysis of the test areas, it was concluded that the training data were satisfactory and that alteration in spectral-cluster assignments would not improve classification accuracy.

DIGITAL CLASSIFICATION OF WATERSHED AREA

The IDIMS CLASFY algorithm uses the training-statistics file and applies a maximum-likelihood decision rule to the Landsat data being classified. Using this rule, each pixel in the image is assigned to the spectral class to which it has the greatest statistical probability or likelihood of belonging. Thus, a new one-band image, called the "classified" image, is created. The Landsat image of the watershed was classified into 35 spectral classes representing 13 Levels II and III resource classes.

To produce the final classification in which the proper resource class is assigned to each classified pixel, the classified image is recoded. Each of the 35 spectral-class pixel values is replaced by a number corresponding to one of the 13 resource classes (fig. 9). Stratification of lowland and agricultural areas is applied in this step by assigning resource-class names to pixels according to their stratum designation. For example, the riparian-hardwoods class (resource class 10) is represented by spectral classes 3, 5, 9, 12, and 18 in the lowland stratum. The relationship between the raw Landsat multispectral data, the classified image (35 spectral classes), and the corresponding 13 Levels II and III resource classes is also graphically displayed in figure 9.

When the recoded output image from CLASFY is displayed on the video screen, the resource classes appear in 13 shades of gray. Each resource class can be color-coded for ease of viewing and evaluation. Figure 13*D* (p. 26) contains an example of the color-coded, classified image showing the 13 Levels II and III classes. Note that, at this reduced scale, it is difficult to distinguish between some of the resource classes owing to their small size and irregular pattern.

For presentation at a relatively small scale (1:250,000 or smaller), it is sometimes desirable to present only the more generalized resource classes. Figure 13*A* shows a color-coded classified image in which the resource classes have been grouped into six Level I classes: forest land, rangeland, rangeland/barren land, wetland, agricultural land, and water.

The results of the classification are presented in table 7, which shows the total area occupied by each of six Level I resource classes, and table 8, which shows the total area occupied by each of 13 Levels II and III resource classes.

ACCURACY OF CLASSIFICATION

Recent publications on Landsat digital classification generally include verification of the accuracy of classification, although the methods used vary greatly. A thoughtful statement of the need for carefully selecting a method for accuracy assessment that fits the

TABLE 7.—*Area summary of digital classification (Level I resource classes) of the Blackfoot River watershed*

Resource class	Number of pixels	Area		Percent of total
		Acres	Hectares	
Forest land	87,055	97,327	39,388	43.4
Rangeland	84,470	94,438	38,219	42.1
Rangeland/barren land	4,280	4,785	1,937	2.1
Wetland	21,581	24,128	9,764	10.8
Agricultural land	2,930	3,276	1,326	1.5
Water	259	290	117	0.1
Total	200,575	224,244	90,751	100.0

TABLE 8.—*Area summary of digital classification (Levels II and III resource classes) of the Blackfoot River watershed*

Resource class	Number of pixels	Area		Percent of total
		Acres	Hectares	
Forest land:				
Conifer	24,483	27,372	11,077	12.2
Aspen	37,825	42,288	17,114	18.9
Mixed conifer/aspen	24,747	27,667	11,197	12.3
Rangeland:				
Sagebrush–perennial grass (high density)	29,541	33,027	13,366	14.7
Sagebrush–perennial grass (medium density)	38,116	42,614	17,246	19.0
Sagebrush–perennial grass (low density)	16,813	18,797	7,607	8.4
Rangeland/barren land:				
Sagebrush–perennial grass (very low density)/strip mines	1,503	1,680	680	.7
Sagebrush–perennial grass (low density)/ strip mines/other disturbed areas	2,777	3,105	1,257	1.4
Wetland:				
Wet meadow	6,607	7,387	2,989	3.3
Dry meadow	12,341	13,797	5,584	6.2
Riparian hardwoods	2,633	2,944	1,191	1.3
Agricultural land:				
Cropland and pasture	2,930	3,276	1,326	1.5
Water:				
Reservoirs	259	290	117	.1
Total	200,575	224,244	90,751	100.0

needs of the potential user was recently made by Heller (1976, p. 20). He comments (emphasis added):

A more thorough analysis of the accuracy of classification maps is needed as are sound statistical sampling procedures to achieve estimates around which a confidence statement can be placed. It is interesting to note that *there exists a heavy reliance on statistical decision theory in classifying multispectral data but an apparent reluctance to use statistical sampling theory to evaluate the results* and provide estimates in a format required by the user community * * * . *It is incumbent on the remote sensing community to make an intensive effort to develop sound sampling procedures to evaluate the accuracy of resource parameters with specific confidence statements based on user objectives.* Map products and tabular data presented in such a manner will gain wider user acceptance and be in a format that allows a resource manager to make a decision on the value of the data and incorporate such data into his management decisions.

Similar sentiments have been echoed recently by Sayn-Wittgenstein and Wightman (1975, p. 1214).

Verification of classification results requires a standard of comparison. Ground data (or "ground truth," as it is often called) may be collected at sample points or over broad areas, thus producing a map of the resource classes that can be compared with the digital classification. However, one can find wide-ranging opinions on whether the map from ground data should be considered completely accurate. Smedes (1975, p. 821) has made some observations that are relevant to this discussion:

Generally, for those classes that can be distinguished from one another by spectral signature or other remote-sensing attributes, the remote-sensing map is more accurate than the ground-truth map. It is a matter of practice that the ground-truth map is upgraded by the remote-sensing map data.

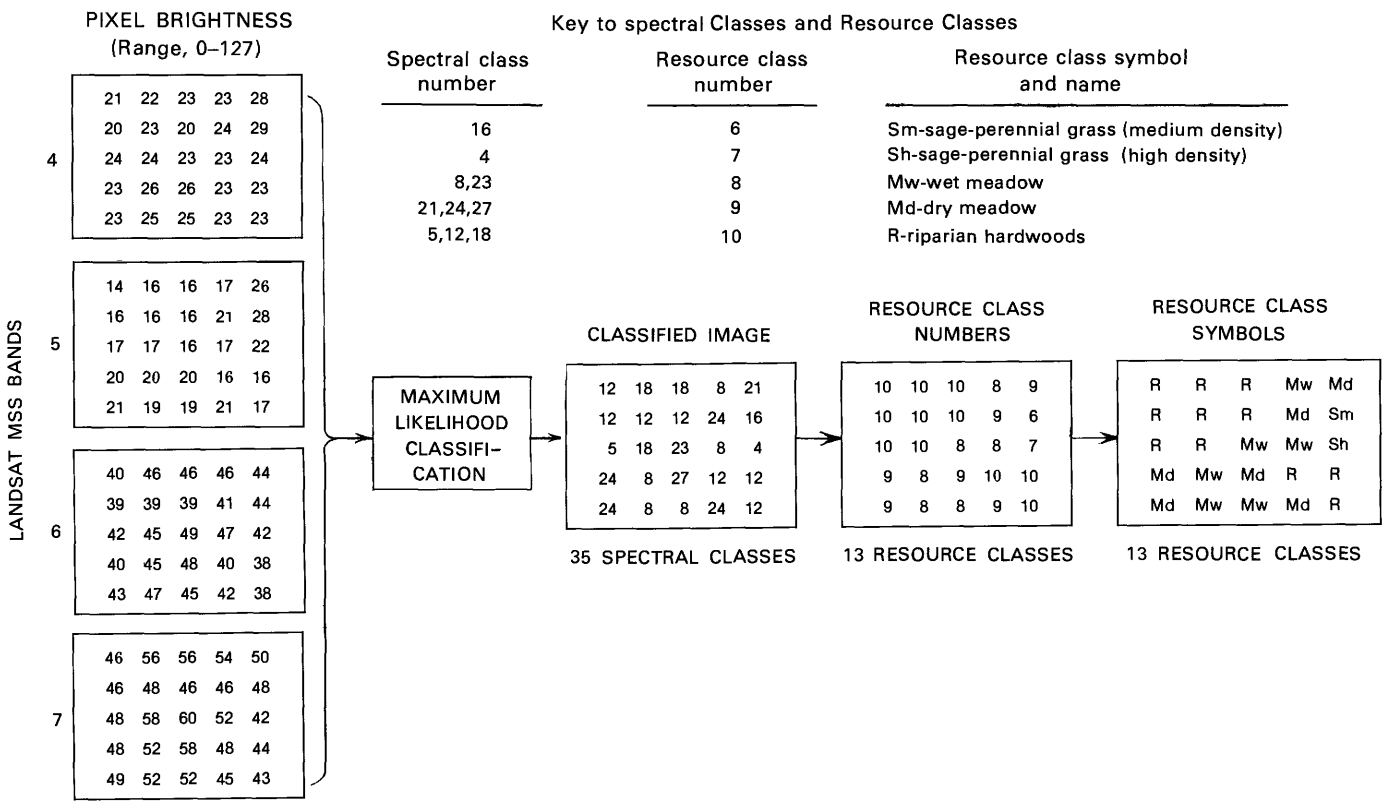

FIGURE 9.—Flow diagram of the digital classification process creating a classified image for a 25-pixel block of Landsat MSS data (4 bands). Spectral-class numbers are assigned to each pixel by the maximum-likelihood classification algorithm. Resource-class assignments (using class numbers and class symbols) corresponding to the spectral classes are shown. The area represented by this 25-pixel block falls within the lowland environmental stratum, and resource-class assignments are made for that stratum.

Reasons for the difficulty of making a nearly perfect ground-truth map of the natural terrain surface include the following * * *: (1) spatial complexity, (2) the problem of mixed terrain classes, and (3) the problem of boundaries * * * .

Williams and Haver (1976, p. 16) offer another point of view:

Even if complete aerial coverage of the desired film-type and resolution were available, there would still be problems because photo interpreter delineations should not be considered as "absolute ground truth" * * * comparisons should be expressed in terms of the percentage of "agreement" and not the percent "correct."

The author's experience, both in this study and elsewhere (Pettinger, 1971), leads him to concur with Williams and Haver's point of view. For purposes of the discussions that follow, accuracy and statements of percent-correct classification will be defined as *agreement* of digital classification with photo interpretation, on a pixel-by-pixel basis.

PIXEL-BY-PIXEL ACCURACY ASSESSMENT

SINGLE-PIXEL METHOD

Two methods for determining digital classification accuracy were discussed earlier: (1) subjective comparison of color video displays of spectral clusters in training areas with corresponding aerial photographs, and (2) comparison of acreage figures for resource classes from digital classification with figures from photo interpretation. Although these methods indicate whether there is general agreement in mapped areas by resource class, they do not indicate how accurately individual pixels were classified. To provide a rigorous assessment of classification accuracy, photo interpretation of the image areas corresponding to single Landsat pixels was compared with the digital classification.[2] As explained earlier, this approach was also desirable for test-area classification, but it was not used because of the extra time and resources that would have been required.

For verification using photo interpretation, pixel boundaries are visually transferred from an enlarged digital image display to an aerial photograph that has been enlarged to a scale at which individual pixels can be plotted. For this purpose, the aerial-photograph scale should be 1:30,000 or (preferably) larger. The accuracy of this transfer will depend on the presence of identifiable landmarks on the photograph and the Landsat display. Photo interpretation of pixel equivalents on the aerial photograph should be made without reference to the digital classification of the pixel, so that the interpreter's decisions are not influenced by his knowledge of the digital classification.

[2] An alternative method of pixel-by-pixel accuracy assessment is to use direct ground observation of pixel areas. For ground verification, one determines the longitude and latitude of a Landsat pixel and plots its position on a topographic map. The map position is visited on the ground and the identity of the ground features at that point is recorded. The major problem with this method is the difficulty in precisely locating the ground equivalent of a single pixel both on the map and in the field. This difficulty is compounded when the terrain is steep and vegetation cover is dense.

PIXEL-BLOCK METHOD

Plotting of single pixels onto aerial photographs is quite difficult, especially in mountainous terrrain or where there are few features for reference. To improve the ease and accuracy of this transfer, blocks of pixels were selected for assessment. The following steps were used to plot and evaluate pixel blocks:

1. By comparing the digital display with the corresponding aerial photograph of the same approximate scale, the corners of each pixel block were plotted on an acetate overlay on the photograph.
2. A network of evenly spaced lines was drawn within the block to define the boundaries of the individual pixels.
3. Each of the pixels was interpreted on the aerial photograph, and the resource class that predominated in the pixel area was identified.
4. The results were compared with the digital classification.

A 5- by 5-pixel block size was selected since it was large enough to overcome some of the difficulties associated with plotting and locating individual pixels yet was small enough to permit a sample of several blocks to be well distributed across the watershed area.

SAMPLE ALLOCATION

The formula used for determining the number of pixels to be sampled in the ith class (n_i) is

$$n_i = \frac{N_i(\hat{p}_i\hat{q}_i)}{(N_i - 1)\frac{E^2}{t^2} + \hat{p}_i\hat{q}_i}, \quad (1)$$

where

N_i = number of pixels classified in the ith class (in the entire watershed),
$\hat{p}_i$ = estimate of proportion of pixels correctly classified in the ith class,
$\hat{q}_i$ = $(1-\hat{p}_i)$,
E = user-specified allowable error, and
t = Student's t-statistic for $n-1$ degrees of freedom at the user-specified probability level.

The sample size for any resource class depends on (1) the total number of pixels classified in that resource class, (2) an estimate of the accuracy of classification for that class, and (3) the user-specified allowable error. The data and results of the calculations made for each class are summarized in table 9.

TABLE 9.—*Sample-size allocation for pixel-by-pixel accuracy assessment*

Resource class	Number of pixels classified (N_i)[1]	Estimate of proportion of pixels correctly classified ($\hat{p}_i$)	Number of pixels to be sampled (n_i)[2]	Number of samples taken
Forest land:				
Conifer	24,483	0.90	35	146
Aspen	37,825	.80	61	162
Mixed conifer/aspen	24,747	.80	61	158
Rangeland:				
Sagebrush-perennial grass (high density)	29,541	.85	49	140
Sagebrush-perennial grass (medium density)	38,116	.75	72	253
Sagebrush-perennial grass (low density)	16,813	.75	72	104
Rangeland/barren land:				
Sagebrush-perennial grass (very low density)/strip mines	1,503	.85	47	47
Sagebrush-perennial grass (low density)/ strip mines/other disturbed areas	2,777	.85	47	50
Wetland:				
Wet meadow	6,607	.90	35	58
Dry meadow	12,341	.90	35	34
Riparian	2,633	.90	34	21
Agricultural land:				
Cropland and pasture	2,930	.80	60	59
Water:				
Reservoirs	259	.97	11	18
Total	200,575	---	619	1,250

[1] From table 8.
[2] Equation (1).

As an example, consider the aspen class. The following values were selected for the input parameters:

N_i = 37,825 pixels classified into the aspen resource class (table 8),
$\hat{p}_i$ = 0.80 (estimated proportion of pixels in the aspen class correctly classified),
E = 0.10 (10 percent error allowed for sample estimate), and
$t_{0.05}$ = 1.96.

From these values, $n_i = 61$. For each resource class, the appropriate N_i value was used, and $\hat{p}_i$ was estimated based on previous experience during the training and testing phases. In all cases, E (0.10) and t (1.96) were constant.

Blocks were randomly selected from the entire image using the IDIMS RANDSAMP algorithm that randomly selects a specified number of blocks of pixels of a specified size (in this case, 5 by 5 pixels). Initially, 30 blocks were chosen in order to satisfy the requirement for a total of 619 pixels in all resource classes. The cumulative total of pixels classified in each resource class was determined from these 750 pixels and compared with the calculated n_i values. Additional random samples were selected until the calculated sample sizes were achieved. In all, 50 blocks were needed to achieve the proper sample size for each class.

PHOTO INTERPRETATION OF PIXEL BLOCKS

The location of each 25-pixel block was plotted on acetate overlays to the high-altitude color-infrared aerial photographs that had been enlarged to an approximate scale of 1:24,000. At this scale, each block measured slightly more than 0.3 in ^{2} (2 cm^2) (fig. 10).

Conventional photo-interpretation techniques (including magnification and stereoscopic viewing) were used to identify the resource class corresponding to each pixel in each block. Where there were mixtures of two or more resource classes in a pixel, the class that occupied the greatest area was identified. Photo-interpretation results were compared with digital classification for Level I (table 10) and Levels II and III (table 11) resource classes. Digital classification results are expressed as a percent of photo-interpretation estimates. Confidence intervals (95 percent probability level) are also given for each resource class and were computed by the following formula (Mendenhall and others, 1971, p. 43–47):

$$\text{C.I. (percent)} = \pm t \sqrt{\frac{p_i q_i \ (N_i - n)}{(n-1) \ N_i}}, \qquad (2)$$

where

p_i = percent of pixels correctly identified in ith resource class,
q_i = $(100 - p_i)$,
N_i = total number of pixels classified in the ith class,
n = number of pixels photo-interpreted in the ith class, and
t = Student's t statistic (= 1.96 at the 0.95 probability level).

Finally, figure 11 contains contingency tables (confusion matrices) that show where disagreements in classification have occurred. For purposes of discussion, disagreements are described as either omission or commission errors. An omission error occurs when a pixel is omitted by digital classification from the correct photo-interpretation class. A commission error occurs when a pixel is incorrectly assigned by digital classification to a wrong class. Thus, an incorrect classification results in both an omission and commission error. A detailed example comparing manual and digital results for a sample 25-pixel block appears in figure 10.

EVALUATION OF RESULTS

Overall agreement of digital classification with manual analysis was relatively low in Levels II and III resource classes (52.2 percent). In only 6 of the 13 Levels II and III resource classes did agreement of digital classification with photo interpretation equal or exceed 60 percent. In all Level I resource classes, agreement was 83 percent. In four of the six Level I resource

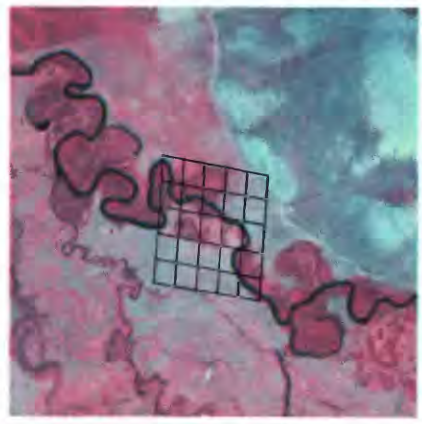

A

APPROXIMATE SCALE

0 ¼ ½ MILE

0 ½ KILOMETER

8	10	10	9	5
10	10	10	9	5
9	10	9	10	9
9	9	9	10	10
9	9	9	9	10

PHOTO INTERPRETATION

B

10	10	10	8	9
10	10	10	9	6
10	10	8	8	7
9	8	9	10	10
9	8	8	9	10

DIGITAL CLASSIFICATION

C

EXPLANATION

RESOURCE CLASS NUMBER	RESOURCE CLASS NAME AND SYMBOL
5	Sl-sagebrush-perennial grass (low density)
6	Sm-sagebrush-perennial grass (medium density)
7	Sh-sagebrush-perennial grass (high density)
8	Mw-wet meadow
9	Md-dry meadow
10	R-riparian hardwoods

DIGITAL CLASSIFICATION

PHOTO INTERPRETATION	Sl	Sm	Sh	Mw	Md	R	Total
Sl		1			1		2
Sm							0
Sh							0
Mw						1	1
Md			1	5	5	1	12
R				1		9	10
Total	0	1	1	6	6	11	25

D

Classification agreement

Resource class number	Level I Number/total	Level I Percent	Levels II and III Number/total	Levels II and III Percent
5			0/2	0
6	1/2	50		
7				
8			0/1	0
9	22/23	96	5/12	42
10			9/10	90
Total	23/25	92	14/25	56

FIGURE 10.—Evaluation of the accuracy of the digital classification of resource data in a 25-pixel block on a Landsat image by comparison with the interpretation of resource classes in a 25-pixel block on a color-infrared aerial photograph. *A*, Color-infrared aerial photograph, including 25-pixel block (reproduced in black and white). *B*, Levels II and III resource-class numbers assigned to each pixel in 25-pixel block, from photo interpretation. *C*, Levels II and III resource-class numbers assigned to each pixel in 25-pixel block, from digital classification. *D*, Contingency table comparing the photo interpretations and digital classification of Levels II and III resource classes in the 25-pixel block. Numbers inside heavy black line indicate frequency of agreement of the classes; numbers outside the heavy black line indicate frequency of disagreement.

TABLE 10.—*Single-pixel accuracy assessment of the digital classification of Level I resource classes*

[The accuracy of digital classification is expressed as percent agreement with the results of photo interpretation. Corresponding confidence intervals (C.I.) at the 0.95 probability level are also given]

Resource class	Number of pixels		(1) as a percent of (2)	C.I. (percent)
	(1) Digital classification	(2) Photo interpretation		
Forest land	434	478	90.8	±2.6
Rangeland	391	475	82.3	±3.4
Rangeland/barren land	41	74	55.4	±11.4
Wetland	100	119	84.0	±6.6
Agricultural land	53	86	61.6	±10.3
Water	18	18	100.0	±.0
Total	1,037	1,250	83.0	±2.1

TABLE 11.—*Single-pixel accuracy assessment of the digital classification of Levels II and III resource classes*

[The accuracy of digital classification is expressed as percent agreement with the results of photo interpretation. Confidence intervals (C.I.) at the 0.95 probability level are also given]

Resource class	Number of pixels		(1) as a percent of (2)	C.I. (percent)
	(1) Digital classification	(2) Photo interpretation		
Forest land:				
Conifer	104	167	62.3	±7.4
Aspen	99	165	60.0	±7.5
Mixed conifer/aspen	68	146	46.6	±8.2
Rangeland:				
Sagebrush–perennial grass (high density)	25	60	41.7	±12.6
Sagebrush–perennial grass (medium density)	170	345	49.3	±5.3
Sagebrush–perennial grass (low density)	17	70	24.3	±10.1
Rangeland/barren land:				
Sagebrush–perennial grass (very low density)/strip mines	16	61	26.2	±11.1
Sagebrush–perennial grass (low density)/strip mines/other disturbed areas	4	[1]13	30.8	±26.1
Wetland:				
Wet meadow	42	51	82.4	±10.6
Dry meadow	21	44	47.7	±14.9
Riparian hardwoods	15	24	62.5	±19.8
Agricultural land:				
Cropland and pasture	53	86	61.6	±10.3
Water:				
Reservoirs	18	18	100.0	±.0
Total	652	1,250	52.2	±2.8

[1]Other disturbed areas only.

classes, there was at least 80 percent agreement with the photo-interpretation results.

Commission errors (for example, classification of nonforest pixels as forest) were more prevalent in resource class Levels II and III than in resource class Level I. For example, there were 205 commission errors in Levels II and III in the conifer, aspen, and mixed conifer/aspen classes (fig. 11*B*). That is, 205 pixels belonging to other resource classes were erroneously classified as either conifer, aspen, or mixed conifer. At this level, this includes misclassification within the three forest classes. In Level I classes, however, there were only 32 commission errors in the forest class (that is, 32 instances where other resource-class pixels were classified as forest).

Greatest spectral variability (as evidenced by frequent commission and omission errors) occurs within the sagebrush–perennial-grass density classes. Significant commission-omission errors also occurred within the forest categories. There were fewer instances of commission and omission for the meadow and riparian-hardwoods classes than in the forest and sagebrush–perennial-grass classes and none in the water class.

At this point, one should consider two factors that affect digital-classification accuracy. The first factor, which contributes to the high number of disagreements in classification in the sagebrush–perennial-grass classes in the lowland environmental stratum, is the 1-year time interval between image dates. Differences in grazing intensity and phenological development of sagebrush–perennial-grass and meadow types from 1974 to 1975 probably lead to real differences in the density-class assignment in these classes.

The second factor affecting digital-classification accuracy is the process of accurately locating the pixels to be verified. Accuracy assessment was made prior to geometric correction of the classified image. Therefore, the Landsat data contain system- and orbit-related errors that affect data geometry. Even though great care was taken to visually determine the location of each 25-pixel block and plot it onto the enlarged aerial photographs, errors occurred in the transfer process. Since Landsat pixels represent a rectangle 1.1 acre (0.44 ha) in area, it will always be difficult to correlate areas within this coarse grid exactly with comparable areas on aerial photographs having much higher resolution. For this reason, there will always be instances in which the photo interpreter is not always looking at the same ground area as did the Landsat sensors.

The following section suggests how ground data were acquired to provide estimates of certain vegetation parameters that provide additional information about the composition of the resource classes.

FIELD DATA COLLECTION

Field sampling was used to acquire data regarding the composition of the vegetation-resource classes. Three pixels were randomly selected from each 25-pixel block used in the photo-interpretation evaluation. Priorities were assigned to blocks so that a variety of upland and lowland environments would be visited. During the 5 days available for field work, 66 pixels from 19 blocks were field checked. The sample size was relatively small, but the field data provide detailed ground characterizations of the resource classes.

Species composition and foliar cover were estimated using a line transect method for the sagebrush–perennial-grass, meadow, and riparian-hardwoods classes. Two line transects were measured per pixel. One line, 150 ft (46 m) in length, was laid out along the

DIGITAL CLASSIFICATION

PHOTO INTERPRETATION	F	S	S/B	T	A	W	Total	Percent agreement
F	434	44					478	90.8
S	28	391	43	13			475	82.3
S/B	1	32	41				74	55.4
T	3	16		100			119	84.0
A		20	13		53		86	61.6
W						18	18	100.0
Total	466	503	97	113	53	18	1250	

A

DIGITAL CLASSIFICATION

PHOTO INTERPRETATION		F			S			S/B		T			A	W		Percent agreement
		Fa	Fm	Fc	Sh	Sm	Sl	Sl/Br Bs	Svl/ Bs	Md	Mw	R	Ag	Wr	Total	
F	Fa	99	37	4	16	5	4								165	60.0
	Fm	28	68	36	10	4									146	46.6
	Fc	10	48	104	3	2									167	62.3
S	Sh	3		1	25	23	7	1							60	41.7
	Sm	18	3	1	69	170	45	10	18	9	1	1			345	49.3
	Sl	2			8	27	17	6	8	2					70	24.3
S/B	Br				1	1	4	4	3						13	30.8
	Svl/Bs	1			2	9	15	18	16						61	26.2
T	Md				3	7	1			21	11	1			44	47.7
	Mw	1			1	2				1	42	4			51	82.4
	R		2		2					1	4	15			24	62.5
A	Ag				3	6	11	11	2				53		86	61.6
W	Wr													18	18	100.0
	Total	162	158	146	143	256	104	50	47	34	58	21	53	18	1250	

B

FIGURE 11.—Contingency tables used to compare the classification of resources in the Blackfoot River watershed by means of photo interpretation with the classification by digital methods. *A*, Frequency of agreement (numbers inside heavy solid line) and disagreement (numbers outside heavy solid line) between Level I resource classes. *B*, Frequency of agreement and disagreement between Levels II and III resource classes. Heavy dashed lines enclose the Level I resource-class frequencies whose totals are shown in A.

topographic contour in the center of each pixel, and a second line of the same length was oriented perpendicular to the first. Ground-cover composition (plant species, soil, or rock) was recorded at 50 sample points along each line. Percent slope and aspect were also recorded.

Within the forest classes, composition, stem diameter, and crown closure were measured in a circular plot, 100 ft (30 m) in diameter, established in the center of each pixel. Trees within the plot were recorded by species and diameter class. Crown closure was also estimated. Other measurements included percent slope, aspect, average height of dominant and codominant trees, stand structure, and general age-class distribution.

Figure 12 illustrates how field data were graphically displayed. In this example, the percent vegetation cover is shown for the 24 sagebrush–perennial-grass pixel areas field-sampled. Cover values for these pixels were grouped according to the density subclass to which they were assigned during photo interpretation. Note that there is overlap in percent foliar cover among the density subclasses. In terms of percent foliar cover, the very-low- and low-density subclasses overlap, as do the medium- and high-density subclasses. The data indicate that it may be more realistic to define two subclasses of sagebrush–perennial-grass type—high and low density.

Although the sample size was small, these data provide added information to quantitatively describe the resource classes. This information, along with other information such as forage production and timber volume, would be required for a multistage inventory of forest and rangeland resources.

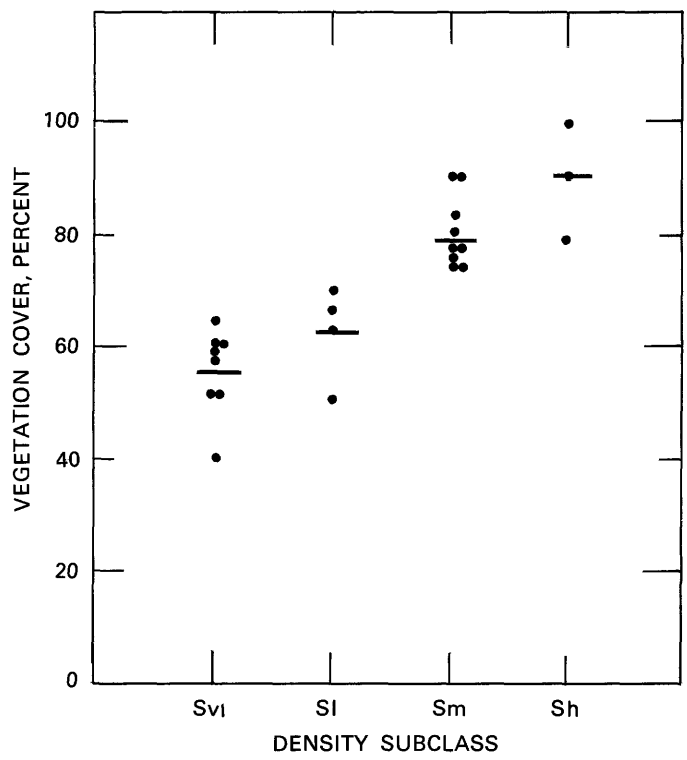

FIGURE 12.—Graphical representation of field data showing percent vegetation cover in 24 randomly sampled pixels from the sagebrush–perennial-grass resource class. Density subclass assignments are from interpretation of high-altitude color-infrared aerial photographs. Horizontal line in each column is the mean value for the subclass.

OUTPUT PRODUCTS GENERATION

Two types of output products were generated: (1) color-coded resource maps (Level I and Levels II and III resource classes) for the entire watershed (scale 1:250,000) and for the area corresponding to the 1:24,000-scale Upper Valley 7½-minute Quadrangle, produced using a film recorder, and (2) a resource map overlay to the 1:24,000-scale topographic map, generated by a computer-driven flatbed plotter.

A spatial-smoothing algorithm was used to improve the appearance of the resource maps and to reduce classification errors. This technique changes the classification for isolated single pixels that may have been misclassified owing to mixing and edge effects related to neighboring resource classes. All output products were geometrically corrected by registering the Landsat data to the corresponding topographic map, either 1:250,000 or 1:24,000 scale. These two operations, spatial smoothing and geometric correction, are described in the following sections.

SPATIAL SMOOTHING

Spatial smoothing, or image reclassification as it is sometimes called, is accomplished using the IDIMS RECLASS algorithm. With this algorithm, the value of each pixel in the classified image is replaced by the value that appears most commonly within a specified window area (block of pixels surrounding the pixel being reclassified) centered on that pixel. For example, if a 3-by 3-pixel window is used, the pixel being reclassified is assigned the value occurring most commonly among the 9 pixels in the window.

Spatial smoothing serves two purposes. First, it is used to remove the "salt and pepper" effect of small inclusions of one or more resource classes that are imbedded in more spatially extensive classes. This effect is frequently caused by misclassification (for example, the classification of a few pixels as mixed conifer/aspen when they actually fall within a pure stand of aspen). Smoothing might eliminate this type of error and produce a more accurate classification. However, if the resource classes are complex and heterogeneous, the "salt and pepper" effect may be an expression of this real

heterogeneity, and smoothing may actually introduce errors.

The second and most important purpose of spatial smoothing is to produce a final classification that has a larger effective minimum map unit than the 1.1-acre (0.44-ha) Landsat pixel. For example, smoothing with a 3- by 3-pixel window can be thought of as imposing a 10-acre (4-ha) minimum mapping unit on the output products. The size of the window used for spatial smoothing should be selected after consideration of the scale of the final map product and its intended use. For example, a large window might be desired for a 1:250,000-scale map that will be used for general resource-planning purposes. A small window might be appropriate for a large-scale resource map.

Two levels of spatial smoothing were applied to data in the Level I and Levels II and III classes before the data were geometrically corrected. In figure 13, the original classifications (*A* and *D*, no smoothing) are to be compared with a 3- by 3-pixel smoothing (*B* and *E*) and 5- by 5-pixel smoothing (*C* and *F*). Since most of the resource classes in the study area are contiguous and relatively homogeneous, a 3- by 3-pixel smoothing appears to improve the map. When used on data in both Level I and Levels II and III resource classes, the 5- by 5-pixel window produces a final product that is so generalized that meaningful map units are lost.

Smoothing alters the number of pixels assigned to each resource class and reduces the number of pixels assigned to classes that represent small, irregularly distributed features such as roads, streams, and very small ponds. The changed pixels commonly are assigned the value of classes that occur in contiguous blocks and constitute a relatively large percentage of the pixels in the study area. For example, the number of pixels in the rangeland/barren-land resource class (table 12) dropped from 2.1 (no smoothing) to 0.9 percent when smoothed with a 5- by 5-pixel window. The pixels in this class occur in scattered, isolated units. However, the reduction in area assigned to the water class (from 259 to 203 pixels) and agricultural-land class (from 2,930 to 2,692 pixels) is not as great because these classes consist of contiguous blocks of pixels that are not reduced significantly in number by the smoothing process. These same relationships hold for the Levels II and III resource classes (table 13).

The decision to perform a smoothing operation, and the choice of the window size to use, should be determined by the distribution and extent of the resource types being classified. For example, if riparian hardwoods (a class of vegetation occurring in narrow bands along stream bottoms) are important in a study of wildlife habitat, then smoothing should be limited to a 3- by 3-pixel window (the smallest-sized window usually applied) or possibly not used.

Smoothing of the data in a color-coded resource map registered to the 1:24,000-scale Upper Valley Quadrangle was also performed (fig. 14); compare with figure 13 for effect of smoothing when displayed at different scales. Before the classification map could be displayed, the image had to be registered to the topographic map using control points. Therefore, geometric correction (see next section) was performed before spatial smoothing was attempted. The degree of smoothing was selected on the basis of information needs, the number of resource classes, and the desired map scale.

GEOMETRIC CORRECTION

Geometric correction involves two steps: (1) generation of transformation coefficients between the Landsat image data and the appropriate topographic map base and (2) registration of the classified image to the map, by a spatial mapping of the image using transformation equations.

To perform the transformation, control points must be selected that are clearly identifiable on both the map and the Landsat image. They should be permanent landscape features, spatially well distributed throughout the image area. Fifteen to 20 points are required to achieve acceptable mapping accuracy (±1 pixel error) on an image 1,024 pixels square. It is wise to select a few extra points because points that have high residual errors might be eliminated during the process of calculating transformation coefficients.

The IDIMS TRNSFORM algorithm reads the image and map control-point pairs, and calculates a first-order transformation matrix using the least-squares method to fit a first-order polynomial. The transformation is applied to the map control points. The calculated coordinates of the points are subtracted from the corresponding image control-point coordinates to provide a measure of the residual errors (table 14). If residual errors for individual points are too high (because of plotting errors or poorly selected control points), these points may be deleted until the mean residual error is acceptable (±1 pixel). New points may be added if the number of points remaining after a series of deletions is less than the suggested limit (15-20), and mean residual errors are still too high. A second-order polynomial can also be used to reduce residual errors because it produces a closer fit to the same number of control points than does a first-order polynomial.

TRANSFORMATIONS FOR BLACKFOOT RIVER WATERSHED TOPOGRAPHIC MAPS

Transformations were performed for both the Preston 1:250,000-scale and Upper Valley 1:24,000-scale maps. A first-order transformation was performed using 26

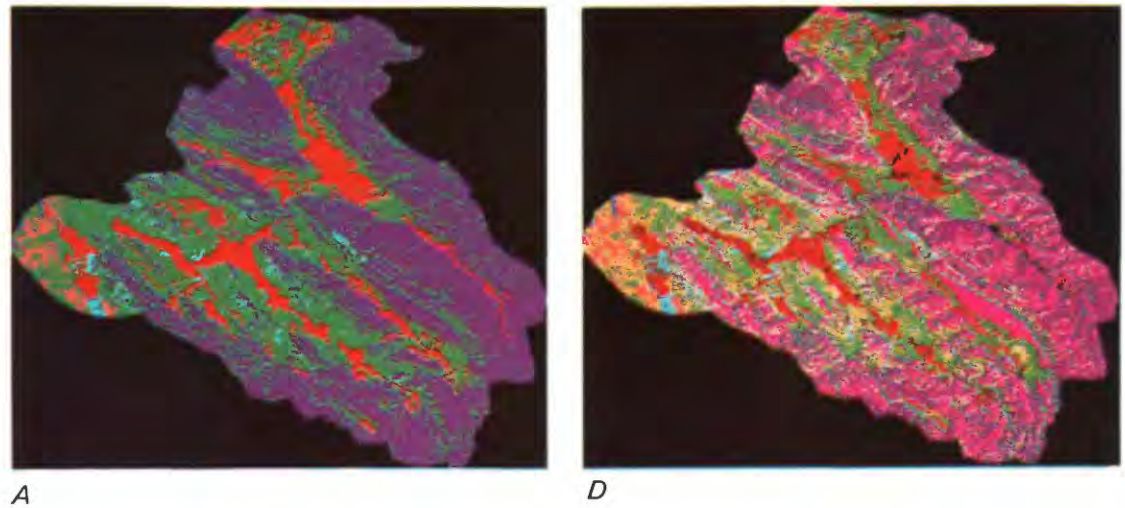

A

D

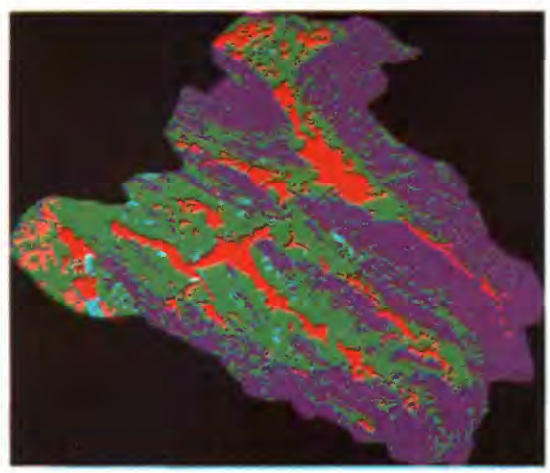

B

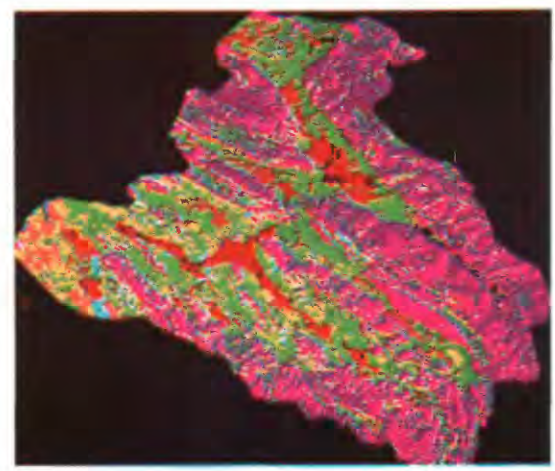

E

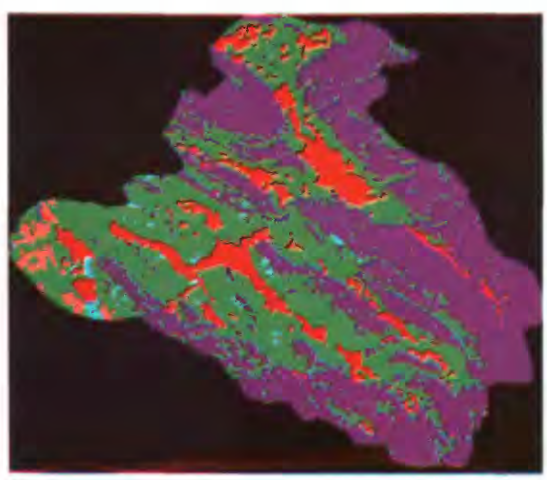

C

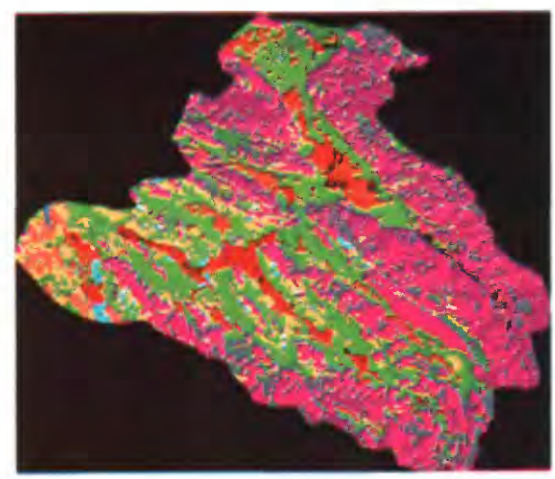

F

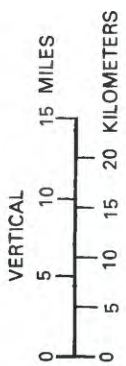
VERTICAL
0
5
10
15 MILES
0
5
10
15
20 KILOMETERS

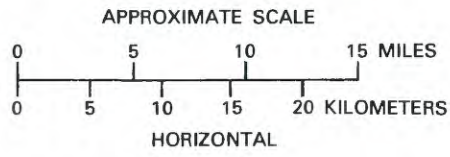
APPROXIMATE SCALE
0
5
10
15 MILES
0
5
10
15
20 KILOMETERS
HORIZONTAL


N

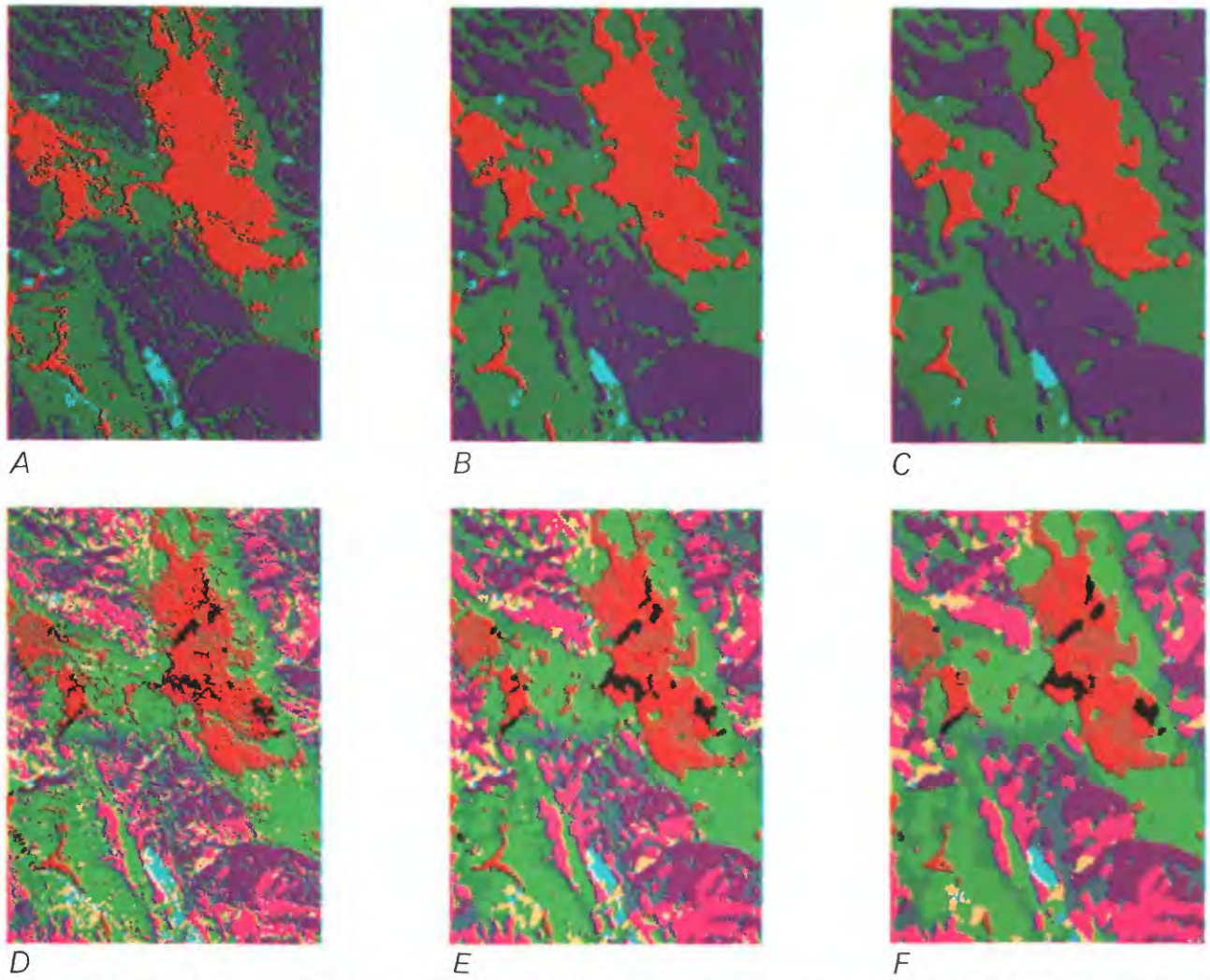

FIGURE 14.—Classified images of a part of the Blackfoot River watershed, geometrically corrected to fit the Upper Valley 1:24,000-scale Quadrangle. *A*, No smoothing (Level I resource classes). *B*, Smoothing with 3- by 3-pixel window (Level I resource classes). *C*, Smoothing with 5- by 5-pixel window (Level I resource classes). *D*, No smoothing (Levels II and III resource classes). *E*, Smoothing with 3- by 3-pixel window (Levels II and III resource classes). *F*, Smoothing with 5- by 5-pixel window (Levels II and III resource classes). Refer to color codes in figure 13.

◀ FIGURE 13.—Classified images of Blackfoot River watershed (IDIMS video displays, not aspect-corrected) showing effect of spatial smoothing with 3- by 3-pixel and 5- by 5-pixel windows. Color assignments for Level I resource classes (*A*, No smoothing; *B*, 3- by 3-pixel window; *C*, 5- by 5-pixel window) are as follows:

Resource class	*Color*
Forest land	Purple
Rangeland	Green
Rangeland/barren land	Light blue
Wetland	Red
Agricultural land	Tan
Water	Dark blue

Color assignments for Levels II and III resource classes (*D*, no smoothing; *E*, 3- by 3-pixel window; *F*, 5- by 5-pixel window) are as follows:

Resource class	*Color*
Forest land:	
Conifer	Purple
Aspen	Violet
Mixed conifer/aspen	Dark gray
Rangeland:	
Sagebrush–perennial grass (high density)	Dark green
Sagebrush–perennial grass (medium density)	Light green
Sagebrush–perennial grass (low density)	Yellow
Rangeland/barren land:	
Sagebrush–perennial grass (very low density)/strip mines	Light blue
Sagebrush–perennial grass (low density)/strip mines/ other disturbed areas	Medium blue
Wetland:	
Wet meadow	Red
Dry meadow	Brown
Riparian hardwoods	Black
Agricultural land:	
Cropland and pasture	Tan
Water:	
Reservoirs	Dark blue

TABLE 12.—*Effect of spatial smoothing on Level I resource classes*

Resource class	No smoothing		Three- by three-pixel window		Five- by five-pixel window	
	Number of pixels	Percent of total area	Number of pixels	Percent of total area	Number of pixels	Percent of total area
Forest land	87,055	43.4	90,122	44.9	92,434	46.2
Rangeland	84,470	42.1	84,031	41.9	83,258	41.6
Rangeland/barren land	4,280	2.1	2,823	1.5	1,855	.9
Wetland	21,581	10.8	20,496	10.2	19,690	9.9
Agricultural land	2,930	1.5	2,780	1.4	2,692	1.3
Water	259	.1	228	.1	203	.1
Total	200,575	100.0	[1]200,480	100.0	[1]200,132	100.0

[1]Does not equal total from the unsmoothed image because boundary pixels from the watershed mask are also reclassified by the smoothing algorithm.

TABLE 13.—*Effect of spatial smoothing on Levels II and III resource classes*

Resource class	No smoothing		Three- by three-pixel window		Five- by five-pixel window	
	Number of pixels	Percent of total area	Number of pixels	Percent of total area	Number of pixels	Percent of total area
Forest land:						
Conifer	24,483	12.2	28,605	14.3	29,158	14.6
Aspen	37,825	18.9	43,631	21.8	45,522	22.9
Mixed conifer/aspen	24,747	12.3	21,502	10.8	20,263	10.2
Rangeland:						
Sagebrush–perennial grass (high density)	29,541	14.7	24,426	12.2	23,866	12.0
Sagebrush–perennial grass (medium density)	38,116	19.0	41,080	20.5	43,460	21.8
Sagebrush–perennial grass (low density)	16,813	8.4	14,665	7.3	11,663	5.9
Rangeland/barren land:						
Sagebrush–perennial grass (very low density)/strip mines	1,503	.7	1,578	.8	1,317	.6
Sagebrush–perennial grass (low density)/strip mines/other disturbed areas	2,777	1.4	1,284	.6	770	.4
Wetland:						
Wet meadow	6,607	3.3	6,710	3.4	6,654	3.3
Dry meadow	12,341	6.2	11,490	5.7	11,390	5.7
Riparian hardwoods	2,633	1.3	2,025	1.0	1,778	.9
Agricultural land:						
Cropland and pasture	2,930	1.5	2,960	1.5	3,177	1.6
Water:						
Reservoirs	259	.1	255	.1	253	.1
Total	200,575	100.0	[1]200,211	100.0	[1]199,271	100.0

[1]Does not equal total from the unsmoothed image because watershed mask boundary pixels are also reclassified by the smoothing algorithm.

control points from the Preston map. After the first iteration, mean residual errors were 4.52 pixels (x) and 2.98 pixels (y). One control point had very high residual errors—34.1 pixels (x) and 10.4 pixels (y)—suggesting that an error was made during the recording of this point. Therefore, this point was deleted, and the transformation was run again. During the second through the seventh iterations, single control points having the greatest residual errors were deleted, one at a time. Care was taken to avoid deleting control points from only one part of the map. Table 14 summarizes the effect (in terms of reducing mean residual errors) of deleting control points. The final result, a second-order polynominal transformation based on 20 control points, resulted in a mean residual error less than one pixel in magnitude.

Eighteen control points were used for the initial first-order transformation of the Upper Valley Quadrangle. Mean residual errors were 1.13 pixels (x) and 0.74 pixel (y). For maps of this scale, mean residual errors of less than one pixel were desired. Hence, the transformation was recomputed until five control points were deleted and the resulting mean residual errors were 0.53 pixel (x) and 0.36 pixel (y).

TABLE 14.—*Mean residual errors after each of eight iterative calculations of transformation coefficients using control points from the Preston 1:250,000-scale map*

Sequence of calculation	Order of transformation	Number of control points	Mean residual error (pixels)	
			x	y
1	First	26	4.52	2.98
2	First	25	1.75	1.44
3	First	24	1.33	1.04
4	First	23	1.18	1.07
5	First	22	.98	1.10
6	First	21	.89	1.06
7	First	20	.80	1.09
8	Second	20	.63	.77

REGISTRATION OF IMAGE TO MAP

The transformation equations were used to perform a spatial mapping of the uncorrected image, producing a geometric correction and rotation of the image so that north is at the top. Output values for the registered images were determined by the nearest-neighbor method. In this resampling technique, the value of a pixel in the transformed (corrected) image is taken from the value of the nearest pixel in the input image.

Separate registrations were produced for matching to the Preston map (entire watershed) and the Upper Valley map (part of the watershed only).

FILM-PRODUCT GENERATION

High-quality film copies of the Level I and Levels II and III resource maps were produced using an Optronics P–1700 film recorder. This device uses digital brightness values to create a black-and-white (positive or negative) film image. Black-and-white positive paper prints of data from single bands were made directly from Optronics film negatives. Multiband positive film images were used to produce false-color composite images by standard photographic techniques. These techniques were used to generate the Landsat images appearing in this publication, including the geometrically corrected classified images (figs. 15, 16). This method produced images of high quality and high color rendition.

Once the color-coded images of the watershed were geometrically corrected and photographically enlarged to match the Preston map, the images could be directly compared with the map. A transparent overlay of the part of the Preston map that includes the watershed can be placed over the classified images, permitting the user to relate the land-cover categories to map features. This is demonstrated in the frontispiece, where the topographic map information is superimposed on the Levels I and II resource classes.

FLATBED-PLOTTER OVERLAY GENERATION

Color-coded overlays to the Upper Valley 1:24,000-scale map were produced using a Calcomp flatbed plotter. Through a series of computer instructions, this device can produce a scaled, inked, translucent map overlay. Each resource class is displayed in a distinctive pattern (fig. 17).

Resource managers prefer this type of output to color-coded classified images (figs. 14, 15, 16) because the resource data can be related to features on a base map. Other resource maps (for example, soils, wildlife habitat, and land ownership) can also be used directly with the resource overlay.

CONCLUSIONS

This study produced vegetation and land-cover maps of the Blackfoot River watershed by computer-assisted classification of Landsat data. The overall classification accuracy (defined as agreement of digital classification with photo interpretation of color-infrared aerial photographs) of the map of Level I resource classes (table 10) was 83.0 ± 2.1 percent (0.95 probability level). Overall classification accuracy for Levels II and III resource classes was 52.2 ± 2.8 percent (0.95 probability level). The map of Levels II and III resource classes had more resource classes (vegetation types) and finer detail than the map of vegetation types required for the EIS on phosphate strip-mining development.

Resource-class maps at scales of 1:250,000 and 1:24,000 were effective output products. Level I classes were most effectively displayed at either scale without spatial smoothing. Levels II and III resource classes were best presented after spatial smoothing with a 3- by 3-pixel window because too much of the original scene detail was lost by using a 5- by 5-pixel window. These conclusions were based largely on the author's knowledge of the resource classes and their spatial distribution within this particular study area, and they did not assume a specific user-defined need. For other environments and particular uses, some other pixel-window size might be desirable.

The man-machine interactive capability of IDIMS facilitated several steps in the analysis process, including training-set selection, environmental stratification, evaluation of classified images, and accuracy assessment. Standard Landsat false-color composites and color-coded classified images were displayed at selected scales on the video screen. Environmental stratification improved discrimination between many upland (aspen, mixed-conifer/aspen, and sagebrush–perennial-grassland) and lowland (wet- and dry-meadow and riparian-hardwood) resource classes that possessed similar spectral signatures.

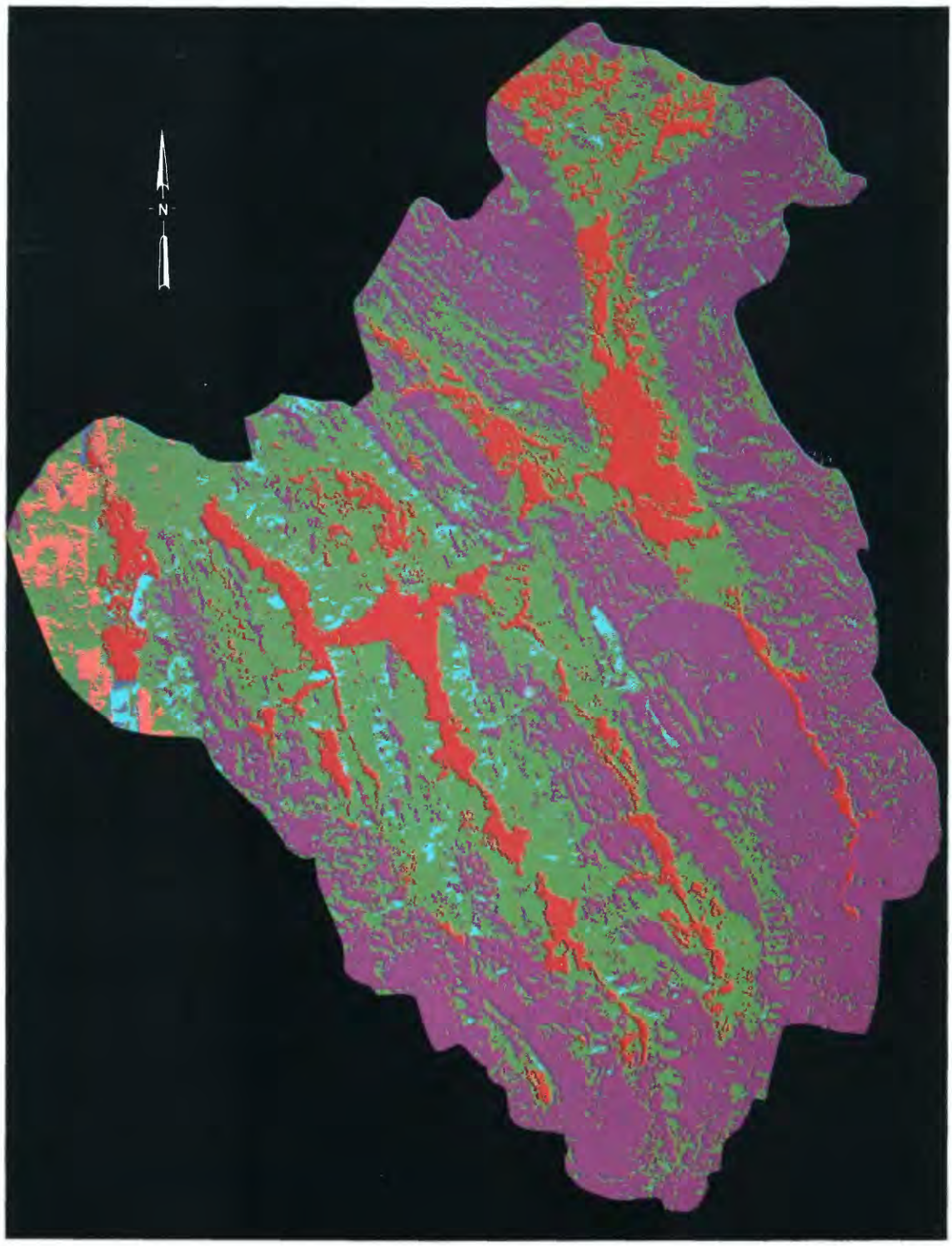

FIGURE 15.–Color-coded classified Landsat image of the Blackfoot River watershed showing Level I resource classes. This image has been geometrically corrected and scaled to match a part of the 1:250,000-scale Preston map. Color codes are as follows:

Resource class	*Color*
Forest land	Purple
Rangeland	Dark green
Rangeland/barren land	Light blue
Wetland	Red
Agricultural land	Tan
Water	Dark blue

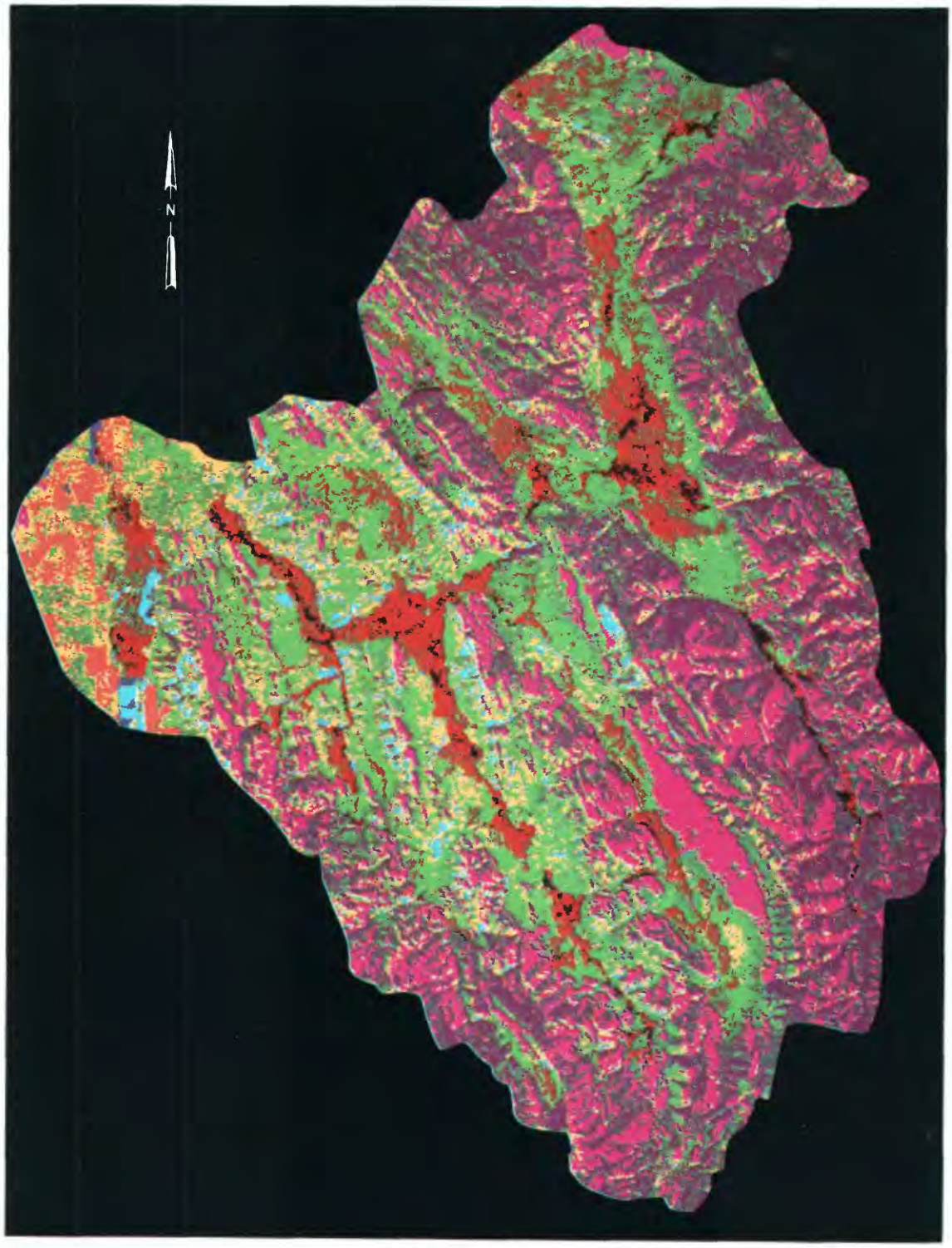

FIGURE 16.–(Caption on following page.)

◀ FIGURE 16.—Color-coded classified Landsat image of the Blackfoot River watershed showing Levels II and III resource classes (no spatial smoothing). This image has been geometrically corrected and scaled to match a part of the 1:250,000-scale Preston map. Color codes are as follows:

Resource class	*Color*
Forest land:	
Conifer	Purple
Aspen	Violet
Mixed conifer/aspen	Dark gray
Rangeland:	
Sagebrush–perennial grass (high density)	Dark green
Sagebrush–perennial grass (medium density)	Light green
Sagebrush–perennial grass (low density)	Yellow
Rangeland/barren land:	
Sagebrush–perennial grass (very low density)/strip mines	Light blue
Sagebrush–perennial grass (low density)/strip mines/other disturbed areas	Medium blue
Wetland:	
Wet meadow	Red
Dry meadow	Brown
Riparian hardwoods	Black
Agricultural land:	
Cropland and pasture	Tan
Water:	
Reservoirs	Dark blue

High-altitude color-infrared aerial photographs were useful for evaluating digital classification accuracy. Most resource classes were easily identified and mapped on the aerial photographs. When greatly enlarged video displays of the Landsat data were compared with the photographs, the location of 5- by 5-pixel blocks could be easily plotted onto the aerial photographs and used to assess classification accuracy.

REFERENCES CITED

Anderson, J. R., Hardy, E. E., Roach, J. T., and Witmer, R. E., 1976, A land use and land cover classification system for use with remote sensor data: U.S. Geological Survey Professional Paper 964, 28 p.

Austin, M. E., 1965, Land resource regions and major land resource areas of the United States (exclusive of Alaska and Hawaii): Washington, D.C., U.S. Department of Agriculture, Soil Conservation Service, Agricultural Handbook 296, 82 p.

Bailey, R. G., 1976, Ecoregions of the United States: Ogden, Utah, U.S. Forest Service [one map].

Carneggie, D. M., and Holm, C. S., 1977, Remote sensing techniques for monitoring impacts of phosphate mining in southeastern Idaho, *in* William T. Pecora Memorial Symposium, 2nd, Sioux Falls, S. Dak., 1976, Proceedings: Falls Church, Va., American Society of Photogrammetry, p. 251–272.

Fleming, M. D., Berkebile, J. S., and Hoffer, R. M., 1975, Computer-aided analysis of LANDSAT-1 MSS data: A comparison of three approaches, including a "modified clustering" approach: West Lafayette, Ind., Purdue University, The Laboratory for Applications of Remote Sensing, LARS Information Note 072475, 9 p.

Heller, R. C., 1976, Natural resource surveys, *in* Congress of the International Society of Photogrammetry, XIII, Helsinki, 1976, Paper, 29 p.

Little, E. L., Jr., 1953, Check list of native and naturalized trees of the United States (including Alaska): Washington, D.C., U.S. Department of Agriculture, Agriculture Handbook No. 41, 472 p.

Mendenhall, William, Ott, Lyman, and Scheaffer, R. L., 1971, Elementary survey sampling: Belmont, Calif., Duxbury Press, 247 p.

Munz, P. A., and Keck, D. D., 1963, A California flora: Berkeley and Los Angeles, University of California Press, 1,681 p.

Pettinger, L. R., 1971, Field data collection—an essential element in remote sensing applications, *in* International Workshop on Earth Resources Survey Systems, Ann Arbor, Mich., 1971, Proceedings: Washington, D.C., National Aeronautics and Space Administration, Office of Space Science and Applications, v. II, p. 48-64.

Rohde, W. G., Miller, W. A., and Nelson, C. A., 1978, Classification of vegetation in the Denali, Alaska, area with digital Landsat data: U.S. Geological Survey Circular 772–B, p. B80–B81.

Rohde, W. G., Taranik, J. V., and Nelson, C. A., 1977, Inventory and mapping of flood inundation using interactive digital image analysis techniques, *in* William T. Pecora Memorial Symposium, 2nd, Sioux Falls, S. Dak., 1976, Proceedings: Falls Church, Va., American Society of Photogrammetry, p. 131–143.

Sayn-Wittgenstein, Leo, and Wightman, J. M., 1975, Landsat applications in Canadian forestry, *in* International Symposium on Remote Sensing of Environment, 10th, Ann Arbor, Mich., 1975, Proceedings: Ann Arbor, Environmental Research Institute of Michigan, v. II, p. 1,209–1,218.

Smedes, H. W., 1975, The truth about ground-truth maps, *in* International Symposium on Remote Sensing of Environment, 10th, Ann Arbor, Mich., 1975, Proceedings: Ann Arbor, Environmental Research Institute of Michigan, v. II, p. 821–823.

U.S. Geological Survey, 1976, Draft environmental impact statement—development of phosphate resources in southeastern Idaho: Reston, Va., U.S. Geological Survey, v. 1, 665 p.

Walker, H. M., and Lev, Joseph, 1953, Statistical inference: New York, Holt, Rinehart, and Winston, 510 p.

Williams, D. L., and Haver, G. F., 1976, Forest land management by satellite: Landsat-derived information as input to a forest inventory system: Greenbelt, Md., National Aeronautics and Space Administration, Goddard Space Flight Center, Information Transfer Laboratory, Intralab Project No. 75–1, 36 p.

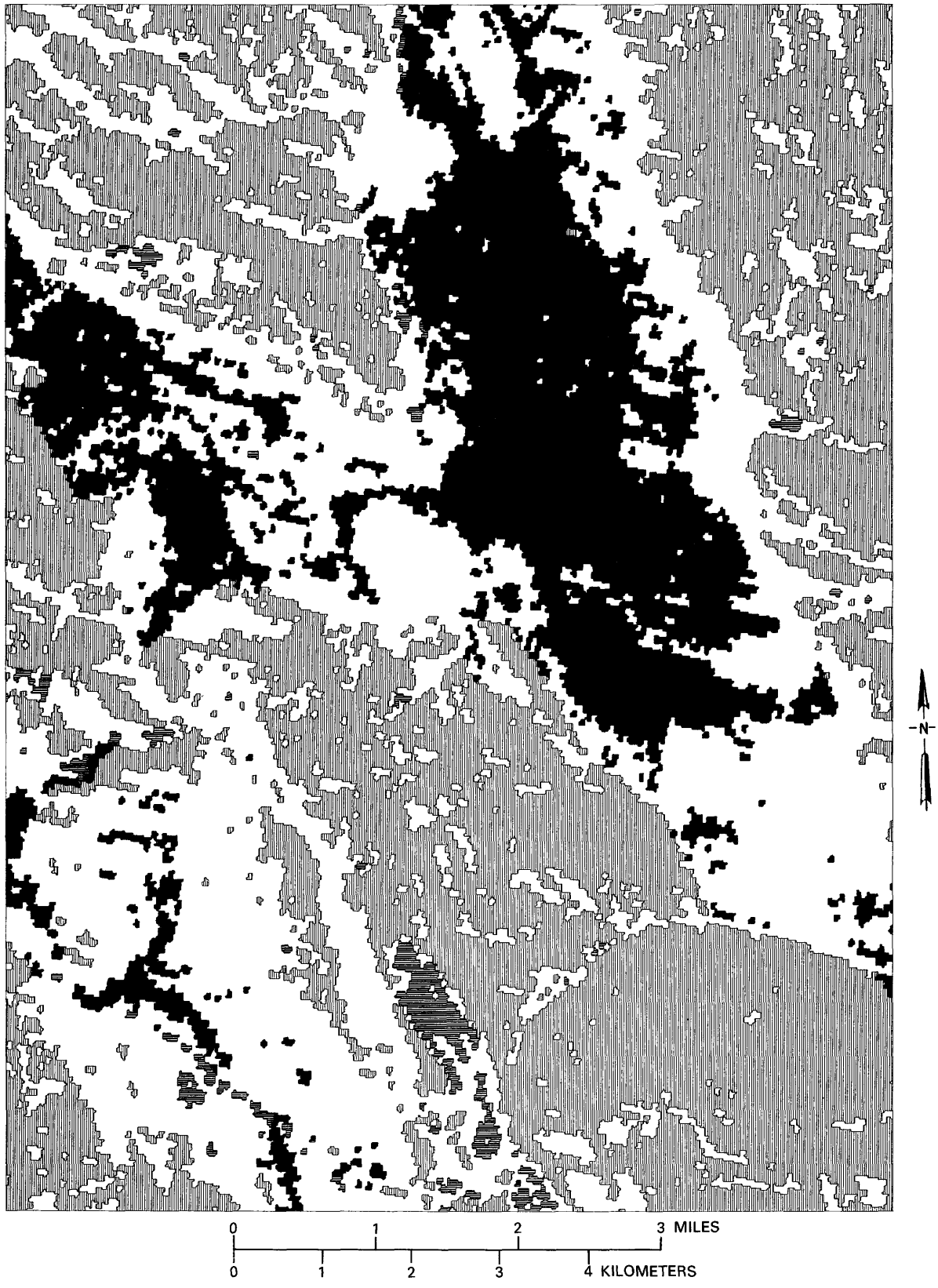

FIGURE 17.—Level I classification of resources in the Upper Valley Quadrangle produced in black and white as an overlay map by a Calcomp flatbed plotter. Although this overlay is reduced in scale here, it was originally produced in color to fit the Upper Valley 1:24,000-scale map. Symbols correspond to the following resource classes: vertical line, forest land; solid black, wetland; blank, rangeland; double horizontal line, rangeland-barren land.